Sortilin mediates vascular calcification via its recruitment into extracellular vesicles

Claudia Goettsch, PhD; Joshua D. Hutcheson, PhD; Masanori Aikawa, MD, PhD; Hiroshi Iwata, MD, PhD; Tan Pham, Anders Nykjaer, MD, PhD; Mads Kjolby, MD, PhD; Maximilian Rogers, PhD; Thomas Michel, MD, PhD; Manabu Shibasaki, PhD; Sumihiko Hagita, PhD; Rafael Kramann, MD; Daniel J Rader, MD; Peter Libby, MD; Sasha A. Singh, PhD; Elena Aikawa, MD, PhD

Supplementary Figure 1 to 16

Supplementary methods

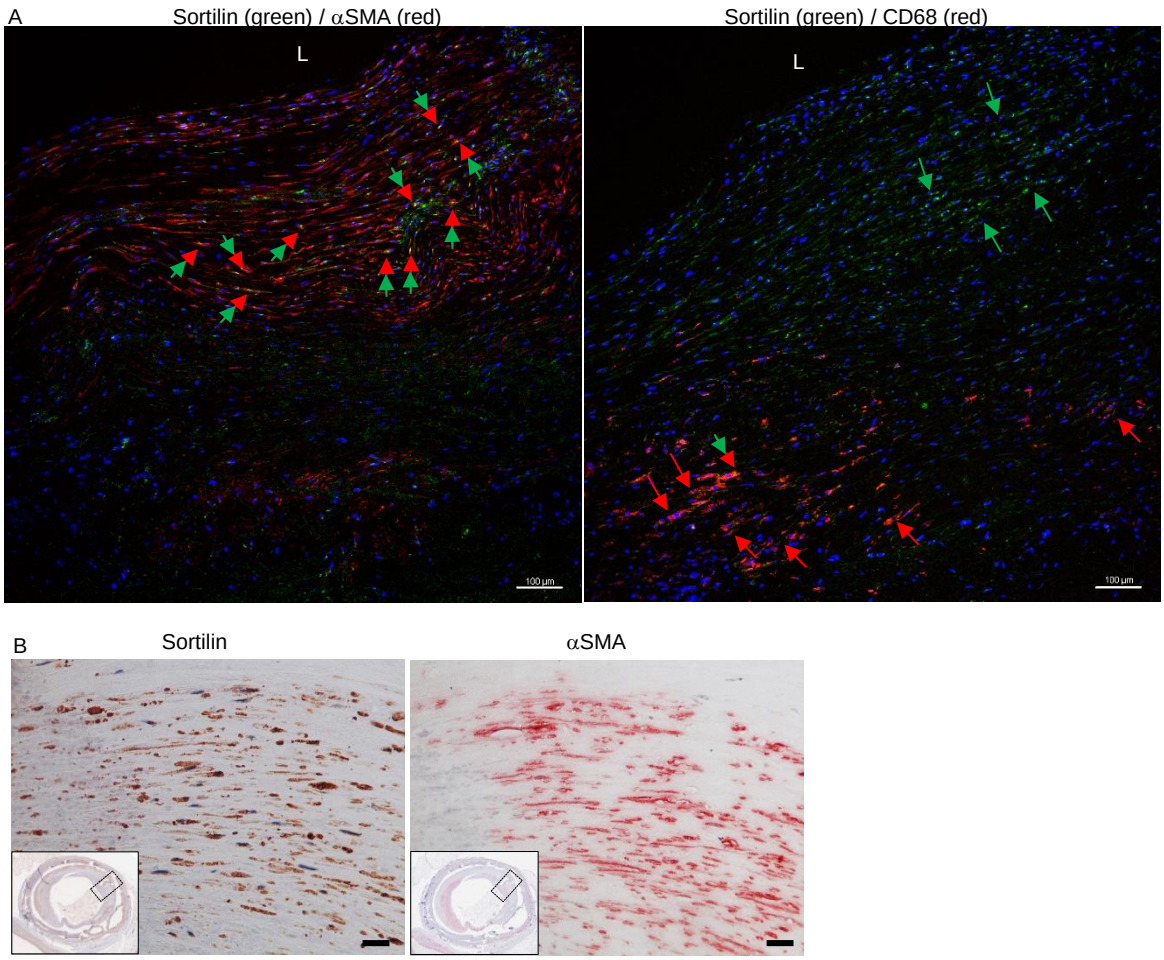

Supplementary Figure 1. Sortilin localizes to αSMA-postive cells in human vascular calcified tissue. (A) Immunofluorescence double staining of sortilin (green)/αSMA (red) or CD68 (red) in human calcified carotid arteries. Arrows indicate the corresponding proteins. Bar=100 µm. **(B)** Decalcified femoral artery from a chronic renal disease patient shows sortilin in SMCs (αSMA). A representative example is shown, n=4. Bar=20 µm.

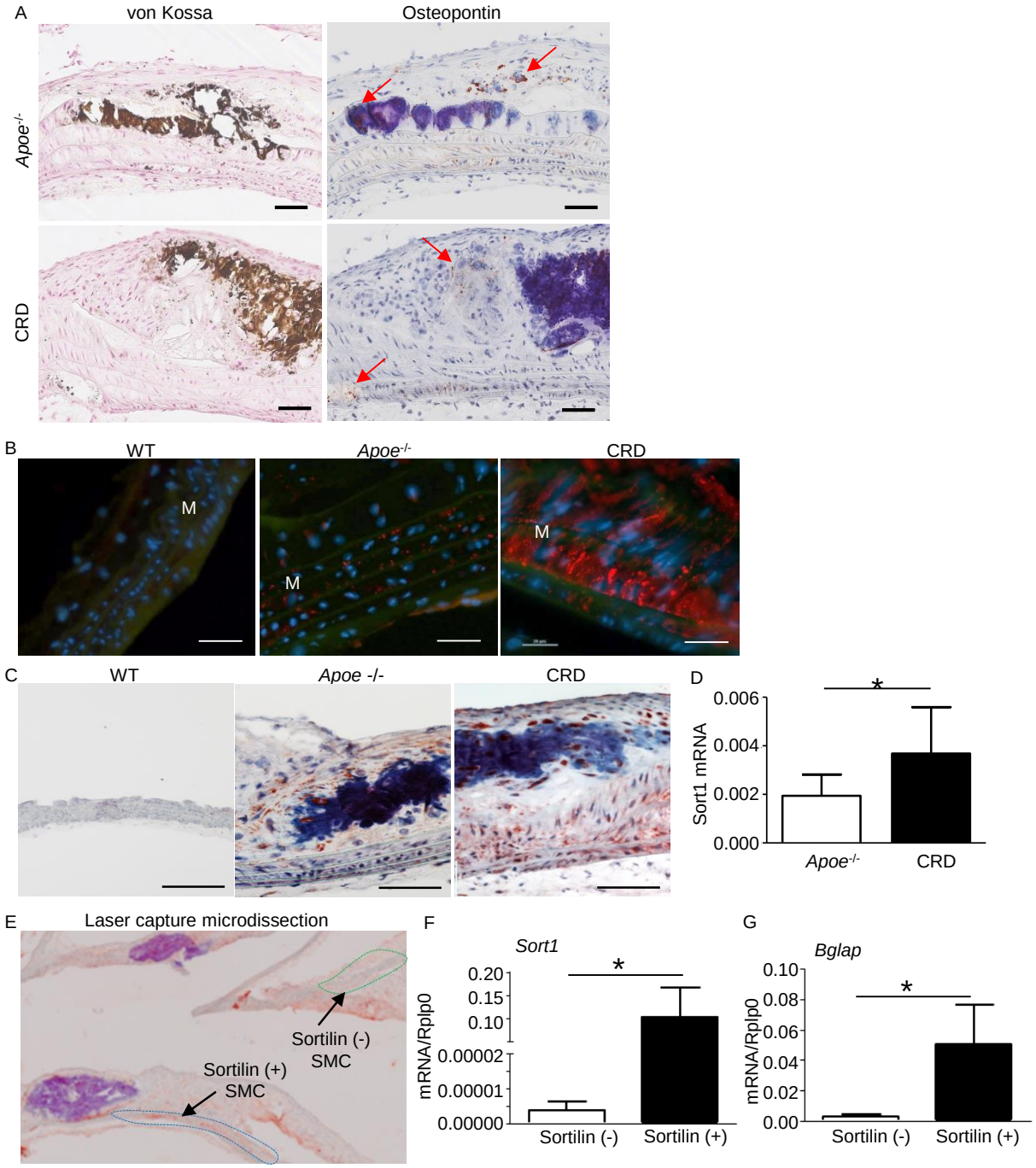

Supplementary Figure 2. Sortilin localizes to calcified tissue from mice. (A) Immunohistochemical staining of osteopontin (red arrow) in aorta of *Apoe*$^{-/-}$ mice without and with CRD. Kossa staining visualizes calcification. One of four animals per group is shown. Bar=100 µm. **(B)** Immunofluorescence staining of sortilin in wild-type (WT), *Apoe-/-* and *Apoe-/-* with CRD mice. Sortilin: red; DAPI: blue; autofluorescence: green. One of four animals per group is shown. Bar=50 µm. M=medial layer. **(C)** Immunohistochemical staining of sortilin in aorta of WT, and *Apoe-/-* mice without and with CRD. One of four animals per group is shown. Bar=100 µm. **(D)** *Sort1* mRNA expression in whole aortic lysates, n=7 (*Apoe*$^{-/-}$), n=9 (CRD). *p<0.05, t-test. Error bars indicate SD. **(E)** Representative image of laser capture microdissection-based sortilin immunostaining. Dotted lines correspond to dissected sections. Purple indicates calcified area. **(F, G)** *Sort1* and *Bglap* (osteocalcin) mRNA levels from sortilin negative (-) and positive (+) SMCs. RNA was isolated from the sections of *Apoe-/-* after cutouts were made using laser capture microdissection (a). n=8 mice. *p<0.05 by Mann Whitney test. Error bars indicate SEM.

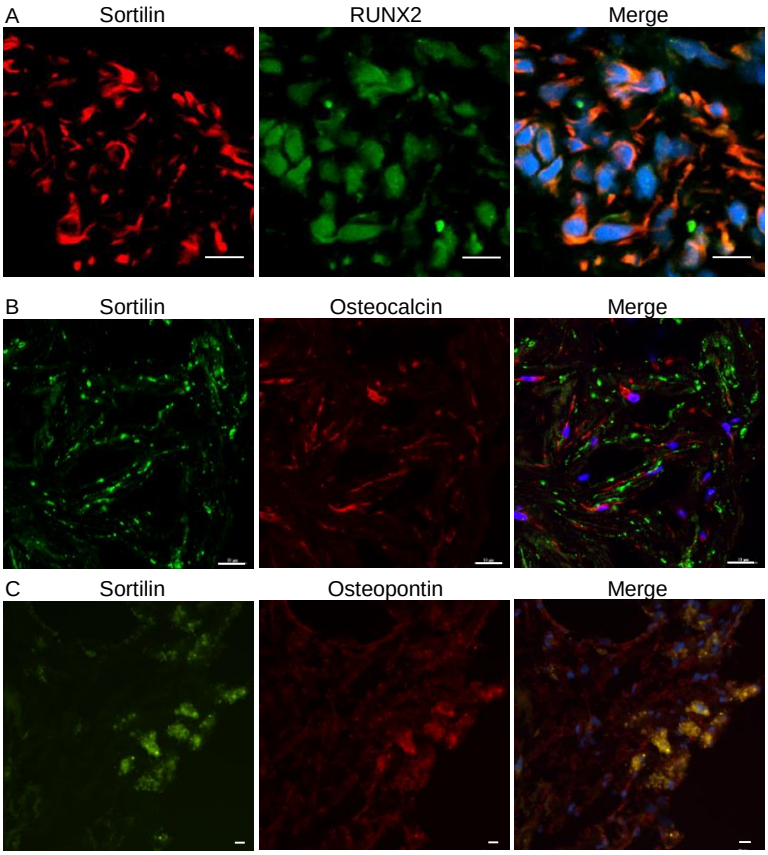

Supplementary Figure 3. SMCs exhibit key osteogenic makers in association with high sortilin expression in calcified human atheroma. Immunofluorescence microscopy of **(A)** sortilin (red) and RUNX2 (green), **(B)** sortilin (green) with osteocalcin (red) and **(C)** sortilin (green) with osteopontin (red) in human calcified lesion. Bar=10 µm.

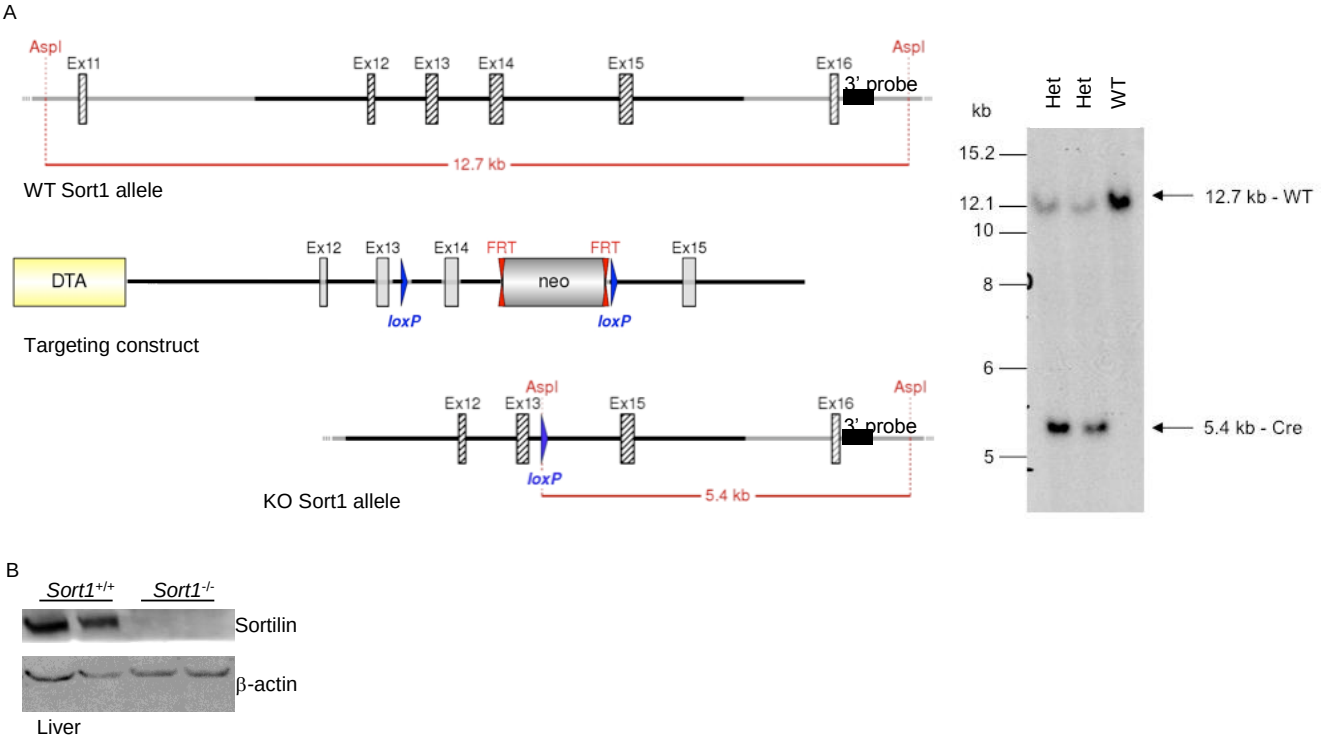

Supplementary Figure 4. Targeting strategy for generation of sortilin-deficient mice. **(A)** Southern blot, performed after excision at *AspI* sites, show 12.7- and 5.4-kb bands in heterozygous knockout (Het) mice but only the 12.7-kb band in WT. LoxP sites are represented by blue triangles and FRT sites by double red triangles. Neo: neomycin positive selection cassette; DTA: Diphtheria toxin negative selection cassette. Diagram is not depicted to scale. **(B)** Western blot of sortilin in liver of WT (+/+) and sortilin-deficient mice (-/-).

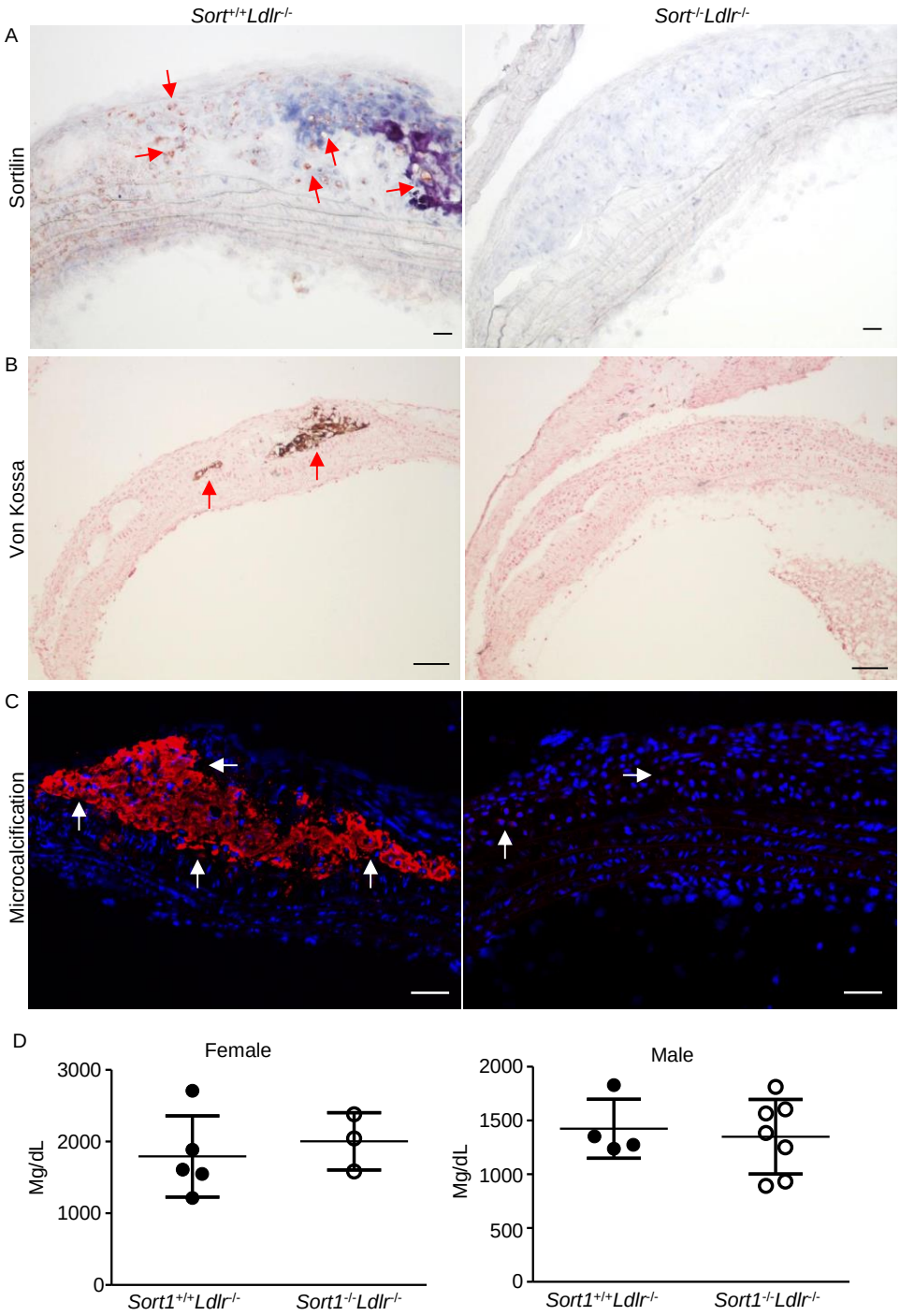

Supplementary Figure 5. Sortilin expression and calcification in plaque regions of *Sort1*$^{+/+}$*Ldlr*$^{-/-}$ and *Sort1*$^{-/-}$*Ldlr*$^{-/-}$ mice that consumed a high-fat, high-cholesterol (1.25% cholesterol) diet for 15 weeks. Representative images of atherosclerotic plaques at the aortic arch lesser curvature stained for **(A)** Sortilin and **(B)** von Kossa for calcium. Bar=100 µm. **(C)** Representative images of microcalcifications (red) using a NIRF calcium tracer. Bar=50 µm. *Sort1*$^{+/+}$*Ldlr*$^{-/-}$ n=7, *Sort1*$^{-/-}$*Ldlr*$^{-/-}$ n=9 for A-C **(D)** Total blood cholesterol does not differ between groups in either female or male mice. Each dot depicts one mouse. Error bars indicate SD. For all sections: *Sort1*$^{+/+}$*Ldlr*$^{-/-}$ (n=5 females, n=4 males), *Sort1*$^{-/-}$*Ldlr*$^{-/-}$ (n=3 females, n=7 males).

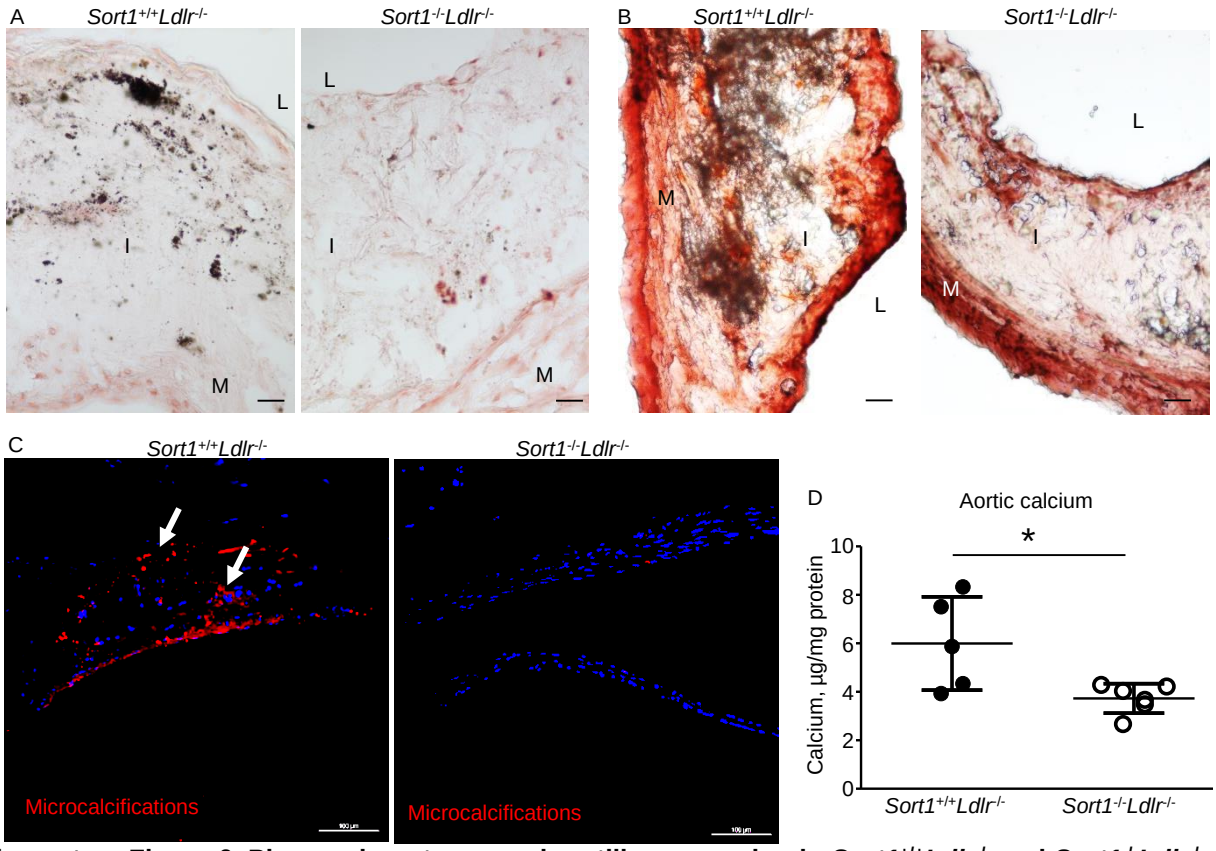

Supplementary Figure 6. Plaque phenotypes and sortilin expression in *Sort1$^{+/+}$Ldlr$^{-/-}$* and *Sort1$^{-/-}$Ldlr$^{-/-}$* mice consuming a Western type diet (0.25% cholesterol) for 32 weeks. Aortic root specimens were prepared. Representative examples from a total of five animals in each group are shown. **(A, B)** Representative images of calcification within the atherosclerotic plaque by von Kossa staining (a) and Alizarin Red S (b). L=lumen, I=intima, M=media. Bar=20 µm. **(C)** Representative images of microcalcifications using a NIRF calcium tracer. Bar=100 µm. **(D)** Quantification of calcification. n=5 per group for B-E. *p<0.05 by t-test. Each dot depicts one mouse. Error bars indicate SD.

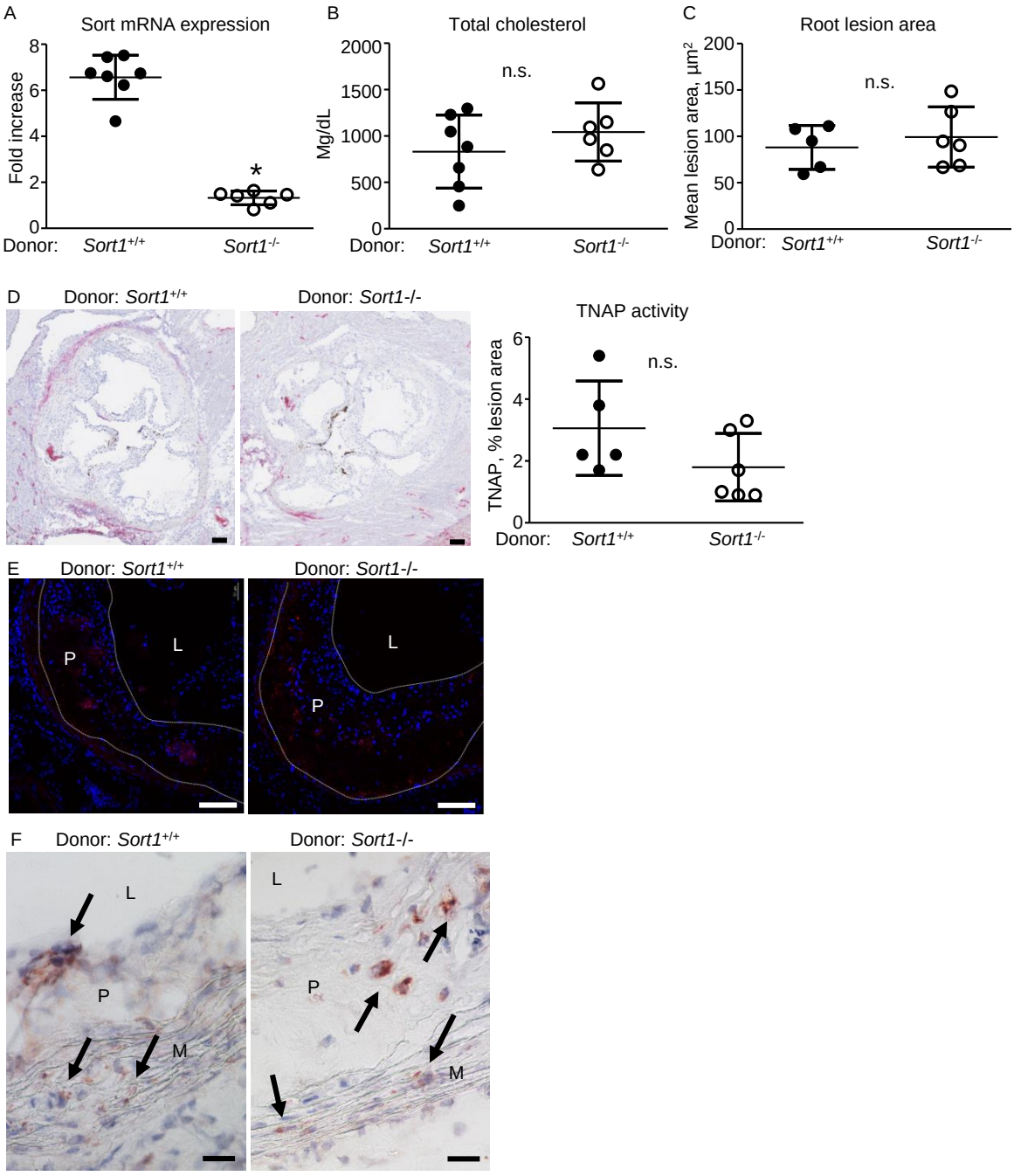

Supplementary Figure 7. Sortilin deficiency in immune cells does not alter vascular calcification. Male *Ldlr*$^{-/-}$ mice (10 week-old) were lethally irradiated and received bone marrow from 10 week-old male *Sort1*$^{-/-}$ or *Sort1*$^{+/+}$ littermate mice and consumed a high-fat high-cholesterol (1.25%) diet for 24 weeks. **(A)** Sortilin mRNA expression in bone marrow cells. Sort1$^{+/+}$ n=7, Sort1$^{-/-}$ n=6. *P<0.05, t-test. **(B)** Plasma cholesterol. Sort1$^{+/+}$ n=6, Sort1$^{-/-}$ n=7. **(C)** Root lesion size. Sort1$^{+/+}$ n=5, Sort1$^{-/-}$ n=6. **(D)** Root plaque TNAP activity. Each dot depicts one mouse. Error bars indicate SD. Bar=200µm **(E)** Representative images of microcalcifications using a NIRF calcium tracer. L=lumen, P=plaque. Bar=100µm. **(F)** Sortilin expression (arrow).M=tunica media. Bar=20µm.

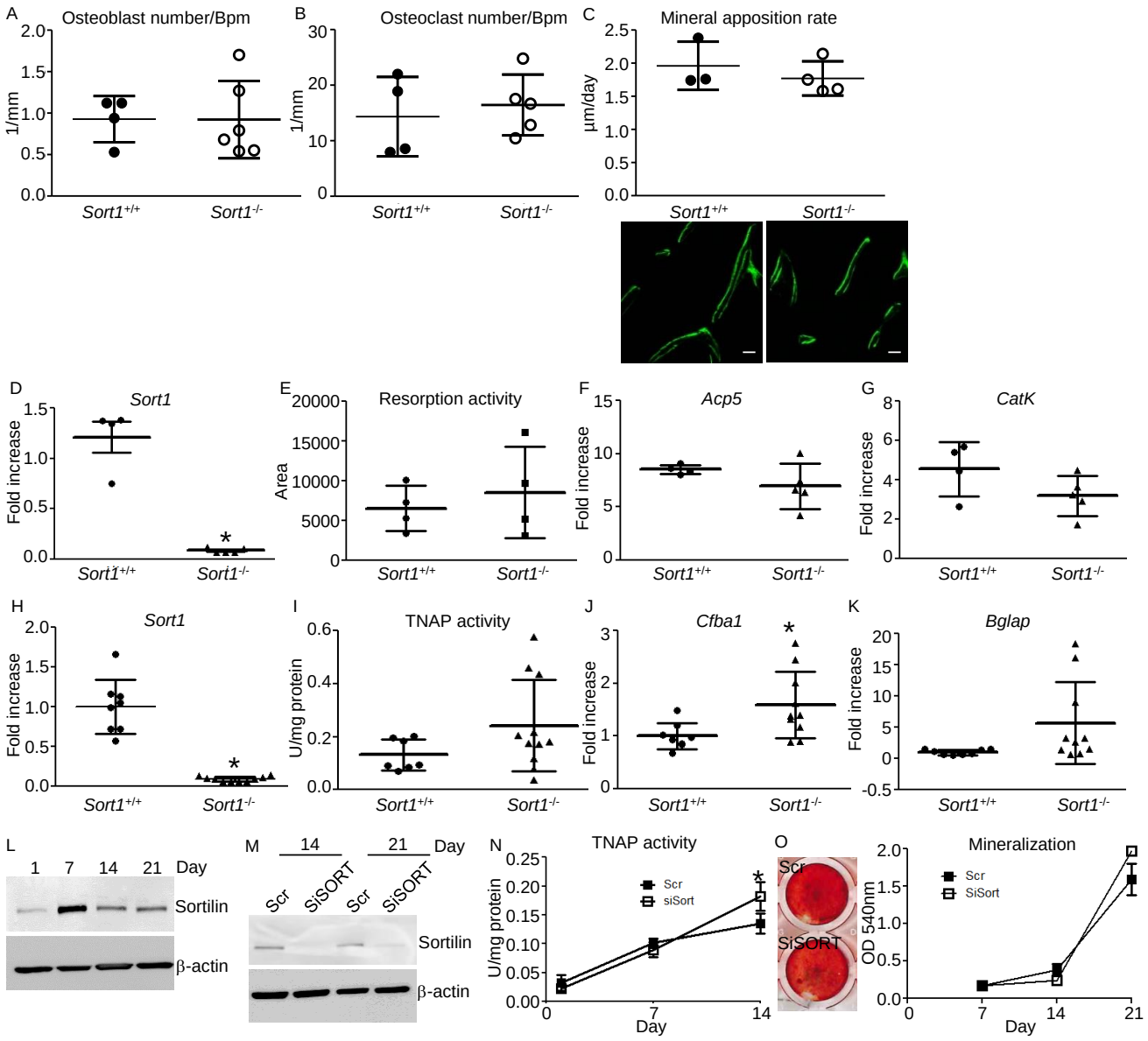

Supplementary Figure 8. Sortilin-deficiency does not alter osteoblast and osteoclast function. (A-C) Static and dynamic histomorphometry of femur mouse bone. Osteoblast **(A)** and osteoclast **(B)** number per bone perimeter of *Sort*$^{-/-}$ mice (n=5-6) and *Sort*$^{+/+}$ mice littermates (n=4). **(C)** Mineral apposition rate in the femur of Sort$^{-/-}$ mice (n=4) and Sort$^{+/+}$ mice littermate controls (n=3). Representative image of calcein-labeled bone. Bar=50µm. **(D-G)** Murine osteoclasts were differentiated from bone marrow stromal cells flushed from femurs using RANKL and M-CSF. n=3 for *Sort*$^{+/+}$, n=4-5 for *Sort*$^{-/-}$. (d) mRNA expression. *P<0.05, t-test. (e) Pit formation assay. **(F, G)** mRNA expression. **(H-K)** Murine osteoblasts were differentiated from bone marrow stromal cells flushed from femurs using osteogenic medium. *Sort*$^{+/+}$ n=7, *Sort*$^{-/-}$ n=10. (H) mRNA expression. *P<0.05, t-test. **(I)** TNAP activity. **(J, K)** mRNA expression. *P<0.05, t-test. **(L-O)** Human osteoblasts were differentiated from human mesenchymal stromal cells using OM. Sortilin was silenced by siRNA (siSORT). Scramble served as control (Scr). n=4 (2 independent cell donors) for L-O. **(L)** Sortilin protein levels at days 1, 7, 14, and 21. **(M)** Sortilin silencing efficiency. **(N)** TNAP activity. *P<0.05, t-test: Scr vs SiSort at day 14. **(O)** Mineralization. Image of representative Alizarin Red S staining at day 21. Quantification of eluated Alizarin Red S at days 7, 14, and 21. Error bars indicate SD.

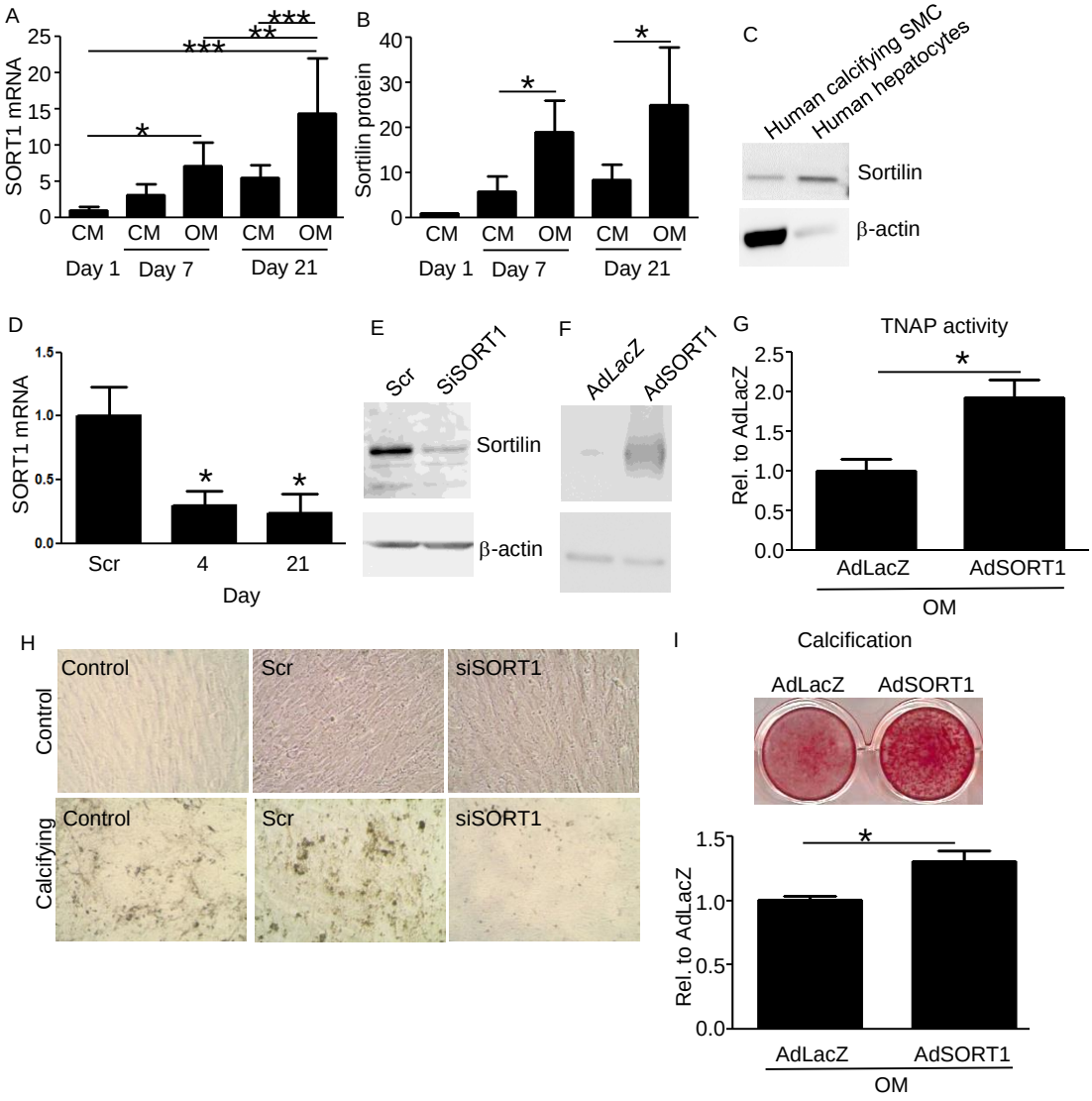

Supplementary Figure 9. Sortlin promotes SMC calcification. (A) SORT1 mRNA expression, relative to day 1. n=4. *p<0.05 **p<0.01 ***p<0.005**,** ANOVA. **(B)** Sortilin protein levels. Statistical analysis from 4 cell donors, relative to day 1. *p<0.05, ANOVA. **(C)** Sortilin protein expression from human calcifying SMCs and human hepatocytes assessed by Western blot. β-actin served as loading control. **(D-I)** hSMCs were cultured up to 21 days in CM or OM. Twice per week during the cell culture period, sortilin was either silenced by siRNA (siSORT1 or scramble control, Scr), or sortilin was overexpressed by adenovirus (AdSORT1). LacZ served as control (AdLacZ). n=3-4 independent hSMC donor for all experiments. **(D, E)** Long-term silencing of sortilin by siRNA suppressed SORT1 mRNA expression by 70% and protein expression by 80%, after 21 days. One of four Western blot images is shown. *p<0.05, t-test vs Scr. **(F)** Sortilin overexpression. β-actin served as loading control. One of four Western blot images is shown. **(G)** TNAP activity at day 14. *p<0.05**,** t-test. **(H)** Representative images of bright field hSMCs showing the nodule formation. **(I)** Calcification at day 21. Top: Representative images of calcification detected by Alizarin Red S-stained mineralized matrix. Bottom: Quantification of eluted calcium. Error bars indicate SD.

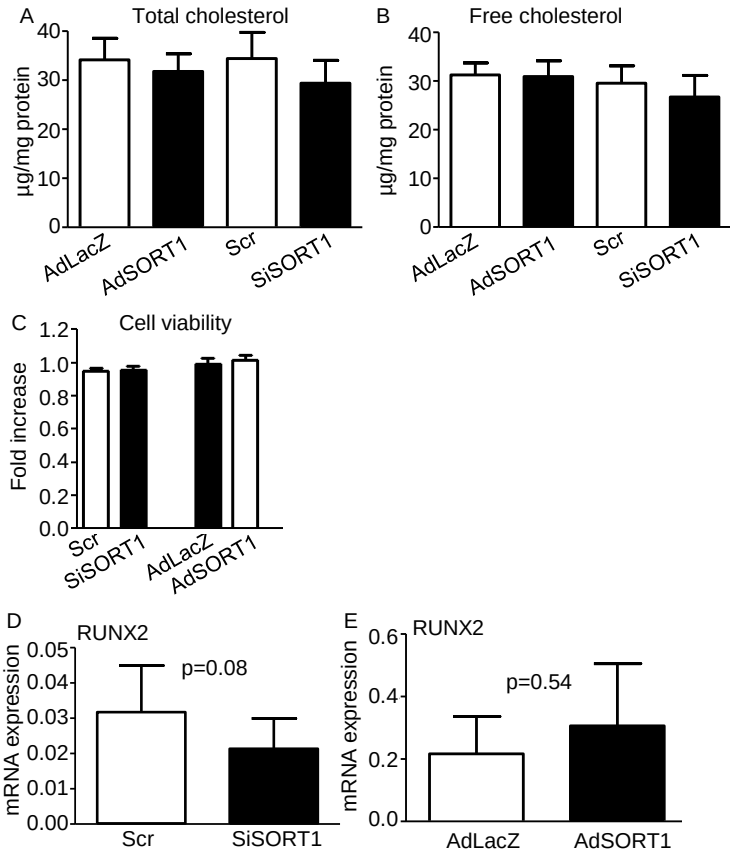

Supplementary Figure 10. Sortilin modulation does not alter cellular cholesterol level, cell viability, and Runx2 levels of calcifying hSMCs. Human SMCs were cultured in OM. Sortilin was either silenced by siRNA (siSORT1 or scramble control, Scr) or induced by adenoviral overexpression (AdSORT1). Total **(A)** and free **(B)** cholesterol. **(C)** Cell viability. **(D, E)** RUNX2 mRNA expression. n=3-4 independent hSMC donors for all graphs. Error bars indicate SD.

A

Sequence	Modification	*m/z*	MH+	RT
SAPGEDEECGR	C9(Carbamidomethyl)	603.73846	1206.46965	7.18
CTSNFLSPEK	C1(Carbamidomethyl)	591.77710	1182.54692	14.27
AAAAGGAFPR		444.73981	888.47234	10.41
TEFGMAIGPENSGK		719.34192	1437.67656	18.88

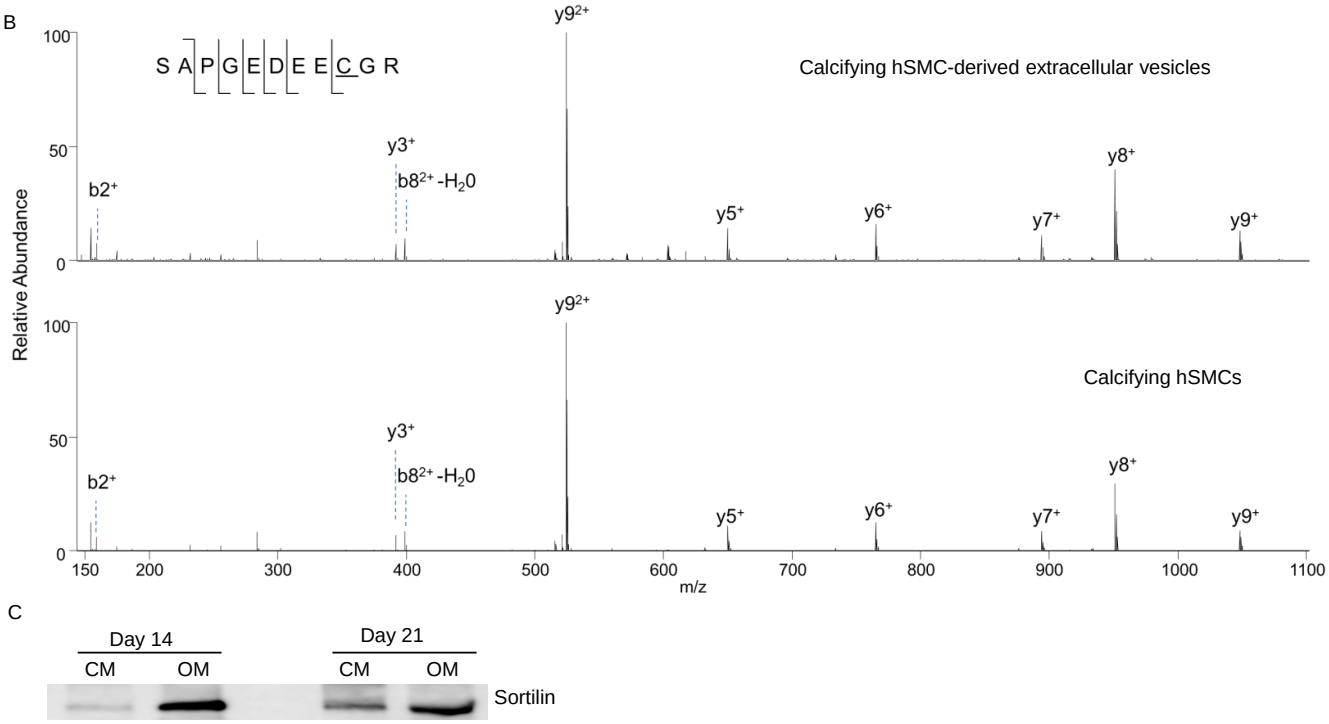

Supplementary Figure 11. Targeted mass spectrometry detects sortilin in extracellular vesicles released from calcifying hSMC. (A) Peptides analyzed using parallel reaction monitoring (PRM) from protein lysate (1 µg) from extracellular vesciles released from calcifying hSMCs. **(B)** MS/MS spectra from an example sortilin peptide observed by PRM (extracellular vesciles released from calcifying hSMCs) or by standard data-dependent acquisition (calcifying hSMCs). **(C)** EVs were isolated from supernatant of hSMC under the adenoviral overexpression of sortilin.

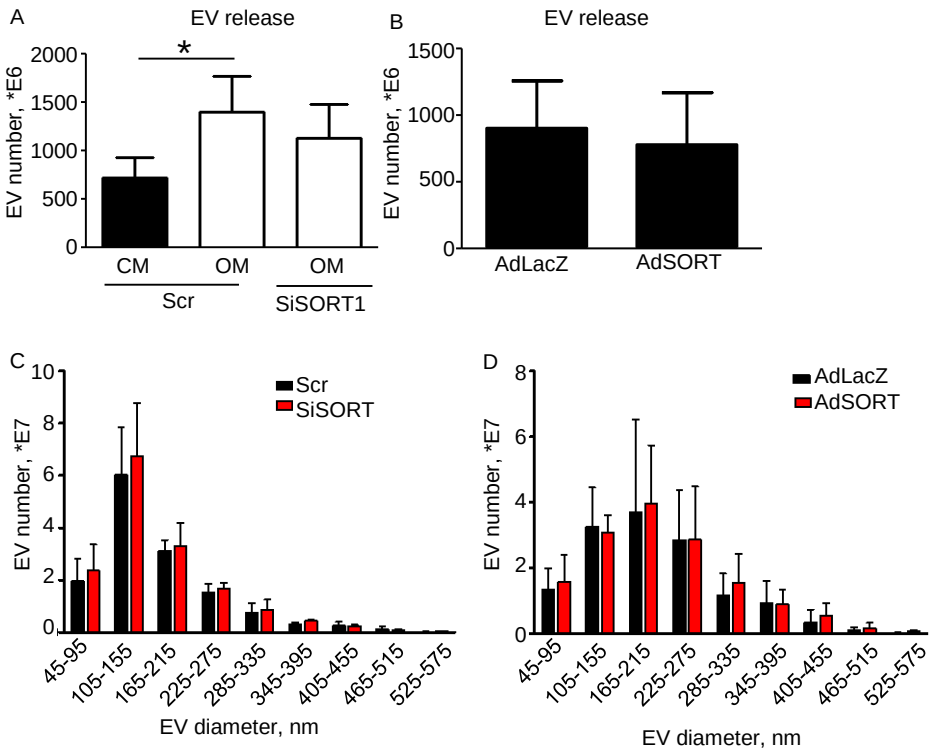

Supplementary Figure 12. Change in cellular sortilin expression do not alter numbers and size patterns of hSMC-released calcifying EVs. The EV number (A, B) and size profile (C, D) was determined in conditioned media of calcifying hSMCs (OM) using nanoparticle tracking analysis. Size is presented in 50 nm increments. **(A, C)** Sortilin silencing in calcifying hSMCs. CM, control media. A, n=4; C, n=3. *p<0.05, ANOVA. **(B, D)** Sortilin overexpression in calcifying hSMCs, n=4. Error bars indicate SD. Each n indicates an independent hSMC donor.

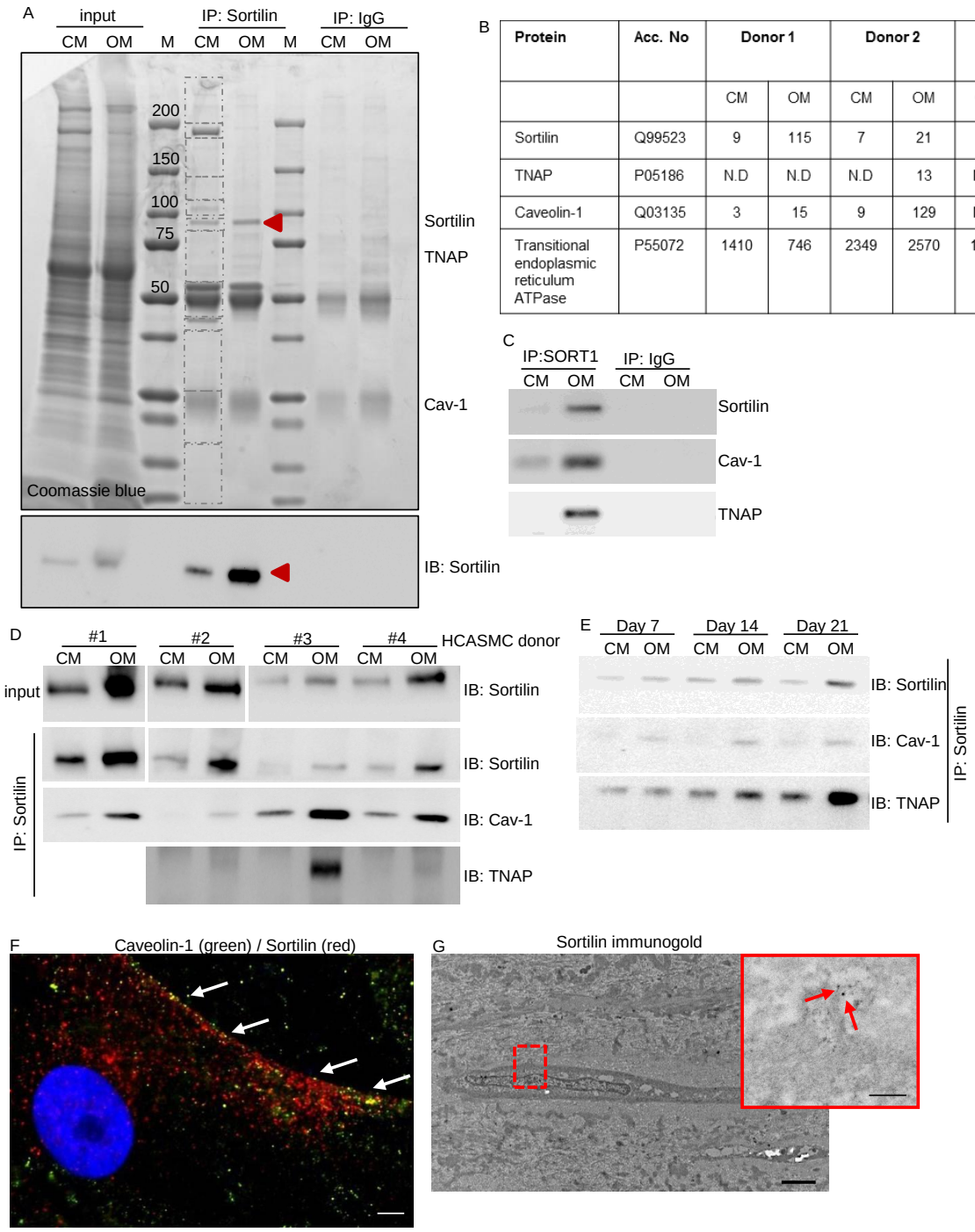

Protein	Acc. No	Donor 1		Donor 2		Donor 3	
		CM	OM	CM	OM	CM	OM
Sortilin	Q99523	9	115	7	21	14	114
TNAP	P05186	N.D	N.D	N.D	13	N.D	34
Caveolin-1	Q03135	3	15	9	129	N.D	135
Transitional endoplasmic reticulum ATPase	P55072	1410	746	2349	2570	1408	1684

Supplementary Figure 13. Mass spectrometric analysis of the sortlin interactome. (A) Sortilin was immunoprecipitated (IP) from control (CM) or calcifying (OM) SMCs cultured for 21 days after IgG-pre-clearance. IgG-IP served as control. One out of three cell donors is shown. Coomassie Blue staining (top) of the gel and Western blot (bottom) of sortilin is shown. Dotted boxes indicate the excised regions of each gel lane. M: size marker in kDa. **(B)** Peptide spectrum matches from 3 independent hSMC cell donors. **(C)** Sortilin was immunoprecipitated (IP) from SMCs cultured for 21 days after IgG-pre-clearance. IgG-IP served as control. One out of three hSMC donors is shown. Western blot for sortilin, caveolin 1 and TNAP. **(D)** Four different hSMC donors support the association of sortilin to caveolin-1 and TNAP. **(E)** Sortilin was immunoprecipitated from hSMCs cultured for 7, 14, or 21 days. **(F)** Immunofluorescence microscopy of sortilin (red) and Cav-1 (green) in calcifying hSMCs (day 21); Bar=50µm. **(G)** Transmission electron microscopy-based immunogold staining of sortilin on human calcified atherosclerotic carotid arteries. One of three samples is shown. Bar=2µm; Inset bar=200nm.

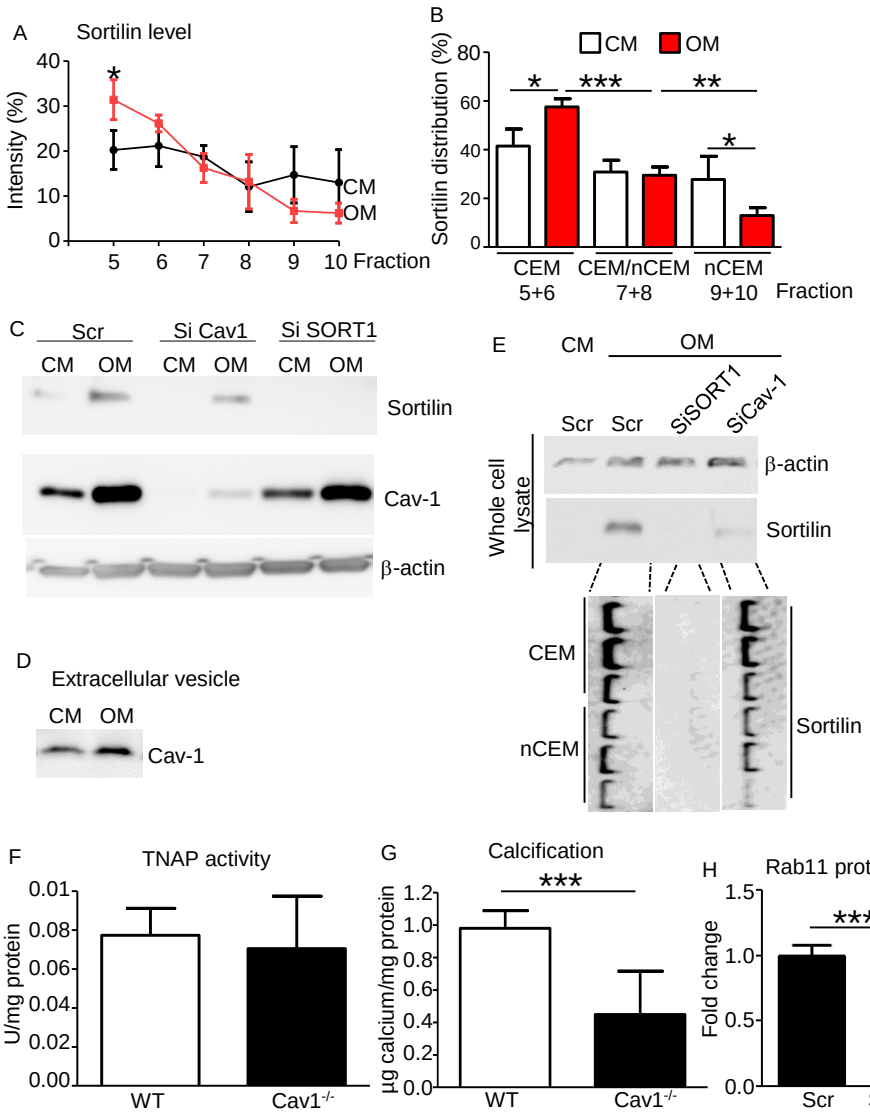

Supplementary Figure 14. Sortilin associates with caveolin-enriched lipid rafts. (A, B) Quantification of sortilin levels in different membrane fractions. hSMCs were cultured for 21 days in CM or OM. Lipid raft/caveolin-enriched membrane (CEM) was resolved from other cellular constituents (nCEM) by a hydrodynamic method. Quantification of Western blot image per fraction (A) and by combining CEM, CEM/nCEM overlapping and nCEM fraction (B). n=3-4. (A) *p<0.05, t-test CEM vs nCEM. (B) *p<0.05 **p<0.01 ***p<0.005, ANOVA. **(C)** hSMCs were cultured for 21 days in CM or OM. Sortilin and caveolin-1 were silenced by siRNA (siSORT1, siCav-1 or scramble control, Scr) twice per week during the entire cell culture period. Protein expression of sortilin, caveolin-1, and β-actin. **(D)** hSMCs were cultured for 21 days in CM or OM. Sortilin and caveolin-1 were silenced by siRNA (siSORT, siCav-1 or scramble control, Scr) twice per week during the entire cell culture period. Western blot of whole cell lysate and CEM/nCEM. One of three independent cell donors is shown. **(E)** Caveolin-1 protein expression in EVs. **(F, G)** hSMCs were isolated from caveolin-1–deficient mice (Cav-1$^{-/-}$) or wild-type (WT) mice and cultured for 14 days (E, TNAP activity) or 21 days (F, calcification) in OM. Mouse SMC isolation from n=4 mice per group. ***p<0.005, t-test **(H)** Rab11 protein expression after Rab11a and Rab11b silencing in calcific SMCs. n=3. ***p<0.005, t-test. Error bars indicate SD.

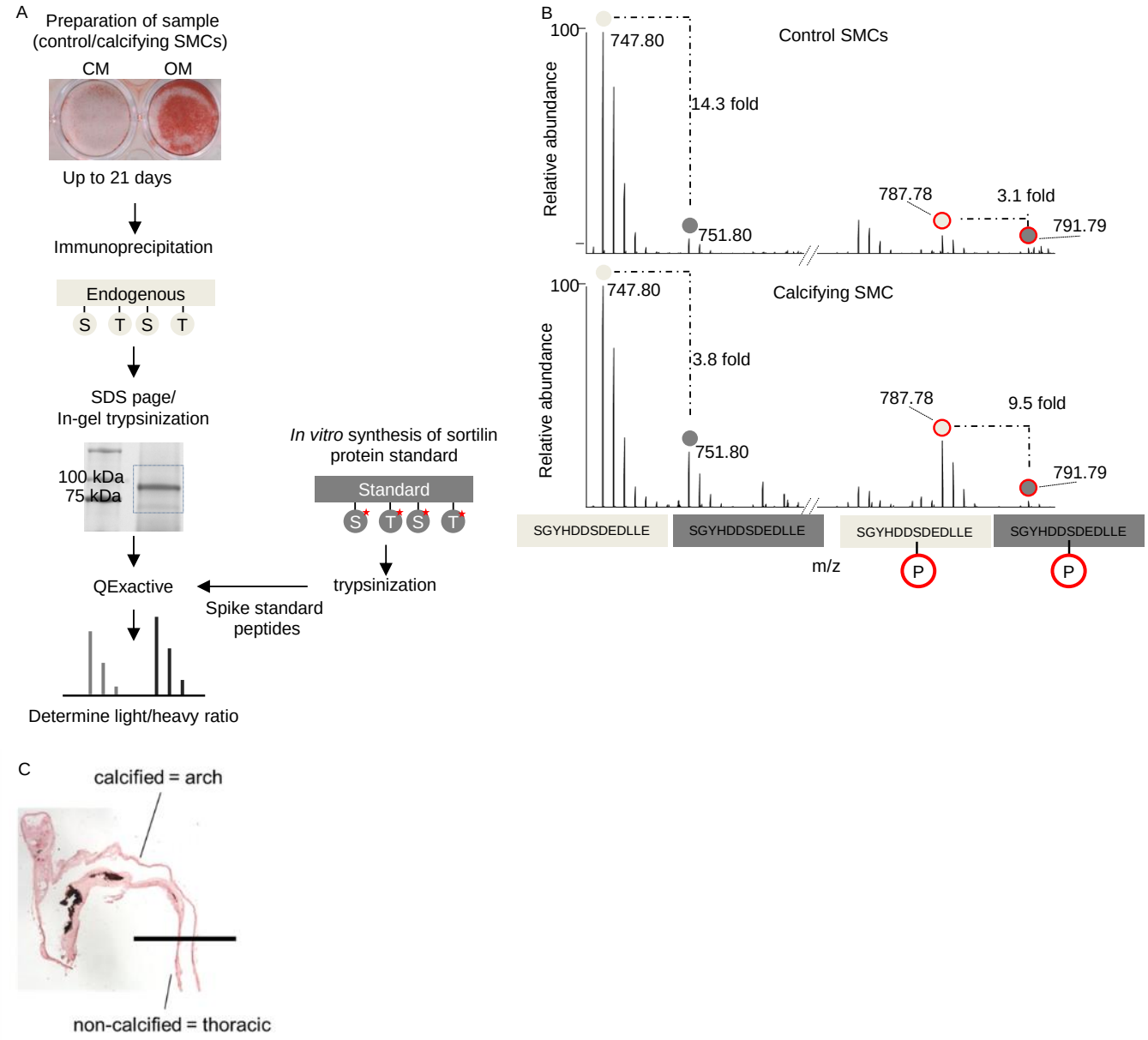

Supplementary Figure 15. A stable isotope labeled sortilin standard enabled targeted proteomics studies. **(A)** Workflow of the quantitative proteomic approach. Trypsinized, *in vitro* synthesized 13C15N-Thr/Ser- labeled sortilin standard was added into trypsinized endogenous sortilin peptides. **(B)** Representative MS1 spectra of the phosphorylated and unphosphorylated forms of SGYHDDSDEDLLE from SMCs cultured for 14 days in CM or OM. SGYHDDSDEDLLE: light (endogenous); 747.80, heavy (standard); 751.80. SGYHDDpS$_{825}$DEDLLE: light, 787.78; heavy, 791.71. **(C)** Von Kossa image to visualize the separation of non-calcified and calcified artery from Apoe$^{-/-}$ mice.

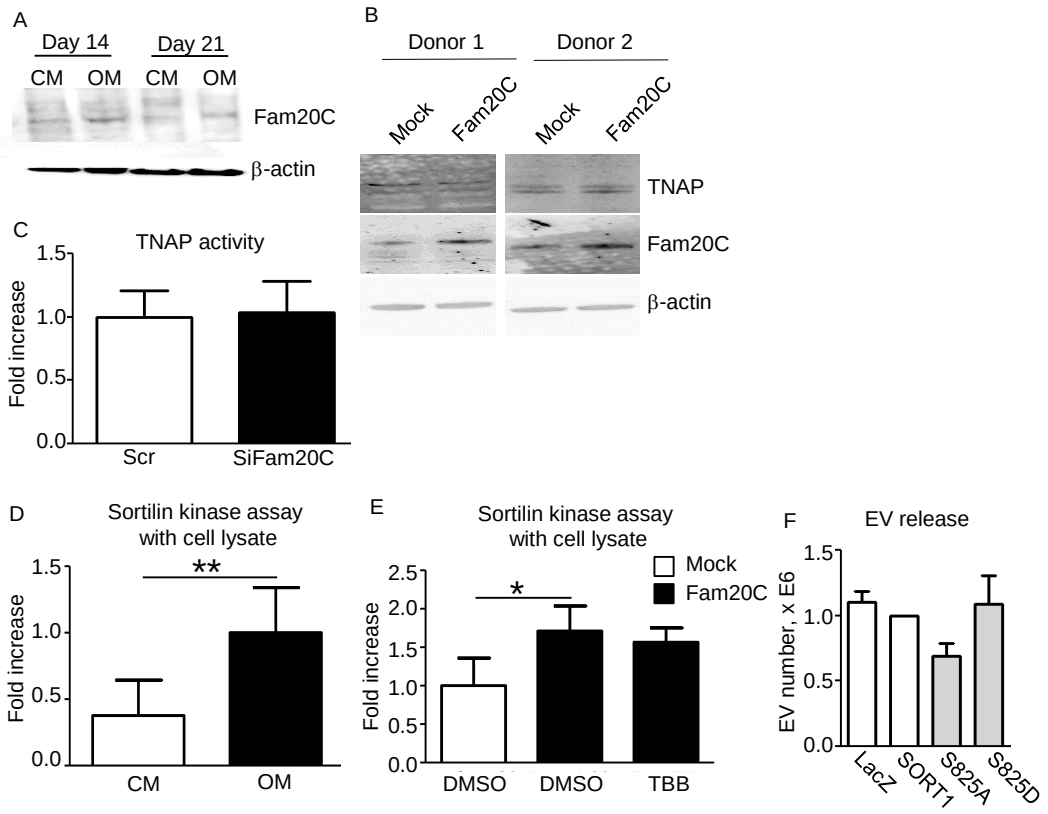

Supplementary Figure 16. Fam20C and CK2 phosphorylate the C-terminus of sortilin. (A) hSMCs were cultured for 14 or 21 days in CM) or OM. Fam20C protein levels determined by Western blot. β-actin served as loading control. **(B)** hSMCs were cultured for 14 days in OM under Fam20C overexpression. Empty vector served as control (Mock). TNAP protein expression by Western blot. Two independent hSMC donors are shown. **(C)** TNAP activity. SMCs were cultured for 14 days in OM. Fam20C was silenced by siRNA (siFam20C or scramble control, Scr). n=3. **(D)** Kinase assay. Cell lysates from CM or OM hSMCs (day 14) were used as a kinase sources for kinase assays with sortilin C-terminal peptide. Calcifying hSMCs exhibit higher kinase activity to phosphorylate sortilin C-terminal peptide. Quantification was done using the MS1 ion signals. n=4. **p<0.01, t-test. **(E)** Kinase assay. Cell lysates from calcifying hSMCs (day14) were used as kinase source for kinase assay with sortilin C-terminal peptide. Fam20C were overexpressed. Empty vector (Mock) served as control. 10 µM TBB were used to inhibit Casein kinase 2. DMSO served as solvent control. Quantification was done using the MS1 ion signals. n=4. *p<0.05, ANOVA. **(F)** EV release. hSMCs were transduced with adenoviral vectors to overexpress sortilin (SORT1) or the different mutated forms (phosphorylation-null S825A; phosphorylation-mimetic S825D). Adenovirus LacZ served as control (LacZ). n=3-4. Each n indicates an independent hSMC donor.

Supplementary Table 1. Sortilin-deficiency does not alter trabecular and cortical bone mass in femur.

	Male		Female	
	Sort$^{+/+}$	*Sort*$^{-/-}$	*Sort*$^{+/+}$	*Sort*$^{-/-}$
Parameter	n=4	n=6	n=3	n=4
Distal femur (trabecular)				
BV/TV (%)	0.18 ± 0.06	0.14 ± 0.03	0.07 ± 0.02	0.08 ± 0.02
Tb.N (1/mm)	5.62 ± 0.36	5.23 ± 0.25	3.79 ± 0.20	3.83 ± 0.46
Tb.Th (mm)	0.043 ± 0.009	0.039 ± 0.005	0.038 ± 0.003	0.039 ± 0.002
Tb.Sp (mm)	0.17 ± 0.01	0.18 ± 0.01	0.26 ± 0.01	0.26 ± 0.04
Bone tissue density (mg HA/cm^2)	823 ± 25.4	825 ± 23.1	815 ± 42.4	819 ± 13.3
BS/BV (mm^2/mm^3)	64.9 ± 13.9	71.6 ± 9.33	78.1 ± 9.17	74.9 ± 5.69
SMI	1.34 ± 0.48	1.62 ± 0.23	2.38 ± 0.22	2.16 ± 0.28
DA	1.68 ± 0.12	1.61 ± 0.10	1.59 ± 0.11	1.66 ± 0.12
Femoral midshaft (cortical)				
Ct.Th (mm)	0.15 ± 0.01	0.16 ± 0.01	0.14 ± 0.02	0.15 ± 0.01
BV/TV (%)	0.89 ± 0.01	0.91 ± 0.01	0.89 ± 0.03	0.89 ± 0.01
Bone tissue density (mg HA/cm^2)	974 ± 37.8	1002 ± 45.1	978 ± 70.9	977 ± 20.8
Ps.Pm (mm)	1.11 ± 0.07	0.98 ± 0.11	0.86 ± 0.05	0.89 ± 0.04
Ec.Pm (mm)	0.96 ± 0.07	0.82 ± 0.12	0.72 ± 0.06	0.74 ± 0.04
J (mm^4)	0.52 ± 0.08	0.41 ± 0.09	0.27 ± 0.04	0.32 ± 0.06

Mice were 10 week-old and consumed a chow diet.
Data were derived from µCT analysis of the distal femur and femoral midshaft. Values represent the mean±SD.
BV/TV, Bone volume/Total volume; Tb.N=Trabecular number; Tb.Th=Trabecular thickness; Tb.Sp=Trabecular separation; BS/BV=Specific bone surface; Conn.D=Connectivity density; SMI=Structural model index; DA=Degree of anisotrophy, Ct.Ar=Cortical bone area; Ct.Th=Cortical thickness; Ps.Pm=Periosteal perimeter; Ec.Pm=Endocortical perimeter; J=Polar moment of interna.

Supplementary Table 2. Sortilin-deficiency in a vascular calcification mouse model does not alter trabecular and cortical bone mass in femur.

	Male		Female	
Parameter	*Sort*$^{+/+}$*Ldlr*$^{-/-}$	*Sort*$^{-/-}$*Ldlr*$^{-/-}$	*Sort*$^{+/+}$*Ldlr*$^{-/-}$	*Sort*$^{-/-}$*Ldlr*$^{-/-}$
Distal femur (trabecular)				
n	2	7	3	3
BV/TV (%)	0.16 ± 0.03	0.15 ± 0.02	0.093 ± 0.030	0.074 ± 0.014
Tb.N (1/mm)	4.59 ± 0.50	4.47 ± 0.28	3.48 ± 0.09	3.31 ± 0.22
Tb.Th (mm)	0.046 ± 0.010	0.047 ± 0.005	0.044 ± 0.007	0.042 ± 0.004
Tb.Sp (mm)	0.21 ± 0.02	0.21 ± 0.02	0.28 ± 0.01	0.29 ± 0.02
Bone tissue density (mg HA/cm^2)	918 ± 5	880 ± 21	895 ± 23	891 ± 51
BS/BV (mm^2/mm^3)	59.9 ± 11.7	59.1 ± 4.3	67.6 ± 13.1	71.1 ± 7.2
SMI	1.44 ± 0.29	1.39 ± 0.24	1.93 ± 0.37	2.23 ± 0.02
DA	1.52 ± 0.07	1.58 ± 0.13	1.58 ± 0.07	1.56 ± 0.08
Femoral midshaft (cortical)				
n	4	7	5	3
Ct.Th (mm)	0.18 ± 0.02	0.17 ± 0.01	0.19 ± 0.01	0.18 ± 0.01
BV/TV (%)	0.92 ± 0.01	0.90 ± 0.11	0.92 ± 0.01	0.92 ± 0.01
Bone tissue density (mg HA/cm^2)	1087 ± 32	1055 ± 16	1051 ± 47	1095 ± 62
Ps.Pm (mm)	0.88 ± 0.05	0.97 ± 0.08	0.88 ± 0.05	0.83 ± 0.01
Ec.Pm (mm)	0.69 ± 0.06	0.80 ± 0.08	0.69 ± 0.04	0.65 ± 0.01
J (mm^4)	0.43 ± 0.08	0.47 ± 0.09	0.41 ± 0.08	0.36 ± 0.01

Mice (10 week-old) consumed a high-fat high-cholesterol diet for 15 weeks.
Data were derived from µCT analysis of the distal femur and femoral midshaft. Values represent the mean±SD.
BV/TV=Bone volume/Total volume; Tb.N=Trabecular number; Tb.Th=Trabecular thickness; Tb.Sp=Trabecular separation; BS/BV=Specific bone surface; Conn.D=Connectivity density; SMI=Structural model index; DA=Degree of anisotrophy, Ct.Ar=Cortical bone area; Ct.Th=Cortical thickness; Ps.Pm=Periosteal perimeter; Ec.Pm=Endocortical perimeter; J=Polar moment of interna.

Supplementary Table 3: Number of peptides and Peptide spectrum matches (PSM) of enriched proteins associated with sortilin in calcifying human SMCs.

Accession number	Protein name	Donor[a]	CM		OM		Fold increase in OM
			# Peptides	# PSM	# Peptides	# PSM	
Q15149-3	Isoform 3 of Plectin OS=Homo sapiens GN=PLEC - [PLEC_HUMAN]	1	Not detected		201	610	unique
		2			310	1434	
		3			200	574	
P62979	Ubiquitin-40S ribosomal protein S27a OS=Homo sapiens GN=RPS27A - [RS27A_HUMAN]	2	Not detected		7	123	unique
		3			9	107	
Q07065	Cytoskeleton-associated protein 4 OS=Homo sapiens GN=CKAP4 - [CKAP4_HUMAN]	1	Not detected		23	65	unique
		3			18	54	
P21283	V-type proton ATPase subunit C 1 OS=Homo sapiens GN=ATP6V1C1 - [VATC1_HUMAN]	1	Not detected		25	124	unique
		2			8	13	
P51116	Fragile X mental retardation syndrome-related protein 2 OS=Homo sapiens GN=FXR2 - [FXR2_HUMAN]	2	Not detected		16	41	unique
		3			10	25	
P04083	Annexin A1 OS=Homo sapiens GN=ANXA1 - [ANXA1_HUMAN]	2	Not detected		8	19	unique
		3			14	64	
P05186	Alkaline phosphatase, tissue-nonspecific isozyme OS=Homo sapiens GN=ALPL - [PPBT_HUMAN]	1	Not detected		11	34	unique
		2			8	13	
P62873	Guanine nucleotide-binding protein G(I)/G(S)/G(T) subunit beta-1 OS=Homo sapiens GN=GNB1 - [GBB1_HUMAN]	1	Not detected		4	8	unique
		2			6	18	
P07339	Cathepsin D OS=Homo sapiens GN=CTSD - [CATD_HUMAN]	2	Not detected		2	4	unique
		3			13	83	
P07384	Calpain-1 catalytic subunit OS=Homo sapiens GN=CAPN - [CAN1_HUMAN]	2	Not detected		10	20	unique
		3			2	3	
O75477	Erlin-1 OS=Homo sapiens GN=ERLIN - [ERLN1_HUMAN]	1	Not detected		6	17	unique
		2			6	12	
		3			2	2	
Q03135	Caveolin-1 OS=Homo sapiens GN=CAV1 - [CAV1_HUMAN]	1	2	3	3	15	5.0
		2	9	126	10	467	3.7
		3	Not detected		7	135	unique
Q96QR8	Transcriptional activator protein Pur-beta OS=Homo sapiens GN=PURB - [PURB_HUMAN]	1	3	3	4	4	1.3
		2	4	5	4	8	1.6
Q15717	ELAV-like protein 1 OS=Homo sapiens GN=ELAVL - [ELAV1_HUMAN]	1	8	28	12	39	1.4
		3	11	39	12	49	1.3
O00425	Insulin-like growth factor 2 mRNA-binding protein 3 OS=Homo sapiens GN=IGF2BP3 - [IF2B3_HUMAN]	1	20	96	21	96	1.0
		2	3	17	7	23	1.4
		3	7	20	15	61	3.1

IP was performed from SMC lysate.
Application filter: not detected in IgG control, 2 or more peptides, present in two or three independent donors and unique to OM or increased in OM
Donor[a]; independent hSMC donor, CM=control medium, OM=calcifying medium, PSM=Peptide spectral matches

Supplementary Table 4: *In silico* search for potenial kinases that phosphorylate sortilin serine 825. Search input: SGYHDDSDEDLLE

Program	Kinase	Score	Cutoff
GPS 2.1 (1)	CK2	12.2	4.5
	CK2/CK2a	5.8	2.9
	Other-Uniquw/KIS	5.6	5.2
	CK1/CK1a	4.7	1.6
	CK1/CK1	4.1	2.0
	TKL/MLK	3.4	1.9
	AGC/GRK/BARK	2.9	1.6
		Threshold	**Risk-Diff.**
http://ppsp.biocuckoo.org/	CK2	3.6	9.13
	GRK	2.1	4.05
	DNA-PK	1.6	1.89
	CK1	1.2	3.38
	PLK	1.0	2.53

Extended Methods

A list of common reagents

DMEM (Lonza); fetal bovine serum (FBS, Fisher); fetal calf serum (FCS, Fisher); dexamethasone (Sigma Aldrich); penicillin/streptomycin (CellGro Antibiotics); β-glycerol phosphate (EMD Millipore); L-ascorbate phosphate (EMD Millipore); optimal cutting temperature compound (OCT); phosphate buffered saline (PBS, Lonza); Alizarin Red S (Sigma Aldrich); all other reagents were purchased from Sigma Aldrich unless specified otherwise.

Human tissue

Atherosclerotic carotid arteries (n=20) were collected from patients undergoing endarterectomy procedures at Brigham and Women's Hospital according to IRB protocol # 1999P001348. Samples were embedded in optimal cutting temperature compound (OCT) and stored at -80^{o}C until use. Carotid arteries from autopsies were collected within 8-18 hours postmortem interval from Brigham and Women's Hospital according to IRB protocol # 2013P002517/BWH. Chronic renal disease (CRD) femoral arteries were obtained from consented clinical autopsies of dialysis patients (8-10 hours postmortem, dialysis vintage 2-4 years) from RWTH Aachen University, Germany, according to the ethical vote #EK 180/14.

Animal procedures

Sort$^{-/-}$ mice were generated by targeted deletion of 191 bp of exon 14 encoding for part of the β-propeller domain (GenoWay). A 5′ murine Sort1 genomic DNA fragment was isolated from a C57BL/6 DNA BAC library and used to generate a targeting construct containing exon 14 flanked by loxP sites, exons 12, 13, and 15 as homology arms, a negative-selection diptheria toxin A cassette and a positive-selection neomycin cassette flanked by Flippase Recognition Target sites (Supplementary Figure 4A). The targeting construct was electroporated into C57BL/6 embryonic stem cells, recombinant clones identified by PCR and Southern blot analysis, and injected into C57BL/6 blastocysts. Heterozygous mice obtained from germline chimeras were bred with Flp-deletor mice and C57BL/6 Cre-deletor mice to generate heterozygous constitutive knockout mice. Sort-null animals were obtained by intercrossing progeny (Supplementart Figure 4B). *Ldlr*$^{-/-}$ mice were obtained from Jackson Laboratory and bred with *Sort*$^{-/+}$ mice to obtain Sort1 and Ldlr double deficient mice. The breding was performed in our animal factility at Beth Israel Deaconess Medical Center. Experiments were carried out on 10 week-old male and female mice consuming

a high-fat high-cholesterol diet (1.25% cholesterol, D12108C, Research Diets, Inc., New Brunswick, NJ, USA) for 15 weeks. In all experiments littermate control and knockout animals were used.

SMCs were isolated from 10 week old, male WT C57/BL6 mice (Jackson Laboratory) and caveolin-1–deficient mice (Jackson Laboratory) using the collagen digestion method (2). All experiments were approved by and performed in compliance with Beth Israel Deaconess Medical Center's Institutional Animal Care and Use Committee (protocol # 017-2010).

Sort1 and Ldlr-double deficient mice consuming a Western-type diet have been reported previously (3). Experiments were carried out on 6 week-old male mice consuming a Western-type diet (0.25% cholesterol, Altromin Western Diet, Brogaarden, Denmark) for 8 months. The experiments were approved by the Danish Animal Experiments Inspectorate (protocol # J. 2006/561-1206).

No blinding was employed.

For histology, samples (aortic roots and arches) were embedded in OCT compound (VWR) and stored at -80^{o}C until use. Arteries for RNA isolation were snap frozen.

Induction of chronic renal disease

Male apolipoprotein E-deficient (*Apoe*-/-) mice (Jackson Laboratory, Bar Harbor, ME, USA) consumed an atherogenic diet (D12079B; 41% milk fat, 0.2% total cholesterol, Research Diets, Inc., New Brunswick, NJ, USA) from 10 weeks of age. At 20 weeks of age, mice were randomized and underwent either 5/6 nephrectomy using a two-step surgical procedure to create CRD (4) or continued the diet. Briefly, a right total nephrectomy was performed 1 week after a left hemi-nephrectomy. One week after nephrectomy, CRD mice were fed a high-cholesterol diet (1.25% cholesterol, D12108C, Research Diets, Inc., New Brunswick, NJ, USA). At 10 weeks after surgery, mice were sacrificed for histological analysis. Age-matched wild-type (WT) C57/BL6 mice (Jackson Laboratory) served as controls.

Bone marrow transplantation

Recipient mice (*Sort*$^{+/+}$*Ldlr*$^{-/-}$, 10 week-old, males) were lethally irradiated with a total dose of 1000 rads. The next day, unfractionated bone marrow cells (1×10^{6}) from age- and sex-matched *Sort*$^{+/+}$ and *Sort*$^{-/-}$ mice were harvested in phosphate buffered saline (PBS) and administered to each recipient mouse via the tail vein injection. Two donor mice from each group were used for 7 irradiated recipient mice. Mice consumed a high-fat, high-cholesterol diet

(1.25% cholesterol, D12108C, Research Diets, Inc., New Brunswick, NJ, USA) for 24 weeks. Reconstitution of the hematopoietic system was determine by PCR in bone marrow (Supplementary Figure 7A).

Macroscopic Fluorescence Reflection Imaging

Calcification in the aorta was monitored *ex vivo* as described previously (5). A bisphosphonate-conjugated near-infrared fluorescent (NIRF) imaging agent (Osteosense-680 EX, PerkinElmer, Boston, MA) was intravenously injected via tail vein into the mice 24 hours before imaging. After mice were euthanized, the aorta was perfused with saline, dissected and imaged to map the macroscopic NIRF signals elaborated by Osteosense680 (excitation/emission: 668±10/687±10nm) using fluorescent reflection imaging (FRI, Image Station 4000MM, Eastman Kodak Co., New Haven, CT). Quantification was performed using MathLab. A pixel intensity above 4500 was considered as a positive signal. Data are given as Osteosense680 positive area related to total area.

Assessment of bone mass and bone microarchitecture

Micro–computed tomography (μCT) was performed at the Yale Core Center for Musculoskeletal Disorders, Yale School of Medicine, New Haven, CT, USA, using previously published methods (6, 7). In summary, femurs were stripped of soft tissue and stored in 70% EtOH at 4° C. Specimens were analyzed in 70% EtOH by cone beam microfocus x-ray computed tomography using a Scanco μCT-35 instrument (Scanco, Brutissellen, Switzerland). Images were acquired at 55 kVp, with an integration time of 500 msec and an isometric voxel size of 6 μm. Segmentation of bone from marrow and soft tissue was performed in conjunction with a constrained Gaussian filter (support = 1; 3X3X3 voxel window; σ = 0.8) to reduce noise, applying density thresholds of 250 and 420 for the trabecular and cortical compartments of the femur, respectively. Volumetric regions for trabecular analysis were selected within the endosteal borders of the distal femoral metaphysis to include the secondary spongiosa located 1 mm from the growth plate and extending 1 mm proximally, or from within the cortical shell of the third lumbar vertebral body. Cortical morphometry was quantified and averaged volumetrically through 233 serial cross-sections (1.4 mm) centered on the diaphyseal midpoint between proximal and distal growth plates.

Bone histomorphometry

Bone histomorphometry was performed at the Bone Histology/Histomorphometry Laboratory, Department of Orthopaedics and Rehabilitation, Yale School of Medicine, New Haven, CT, USA. Two intraperitoneal injections of calcein (30 mg/kg) were injected 5 and 2 days before sacrifice. After μCT measurement, bones from the right

proximal tibia were fixed in formalin and dehydrated in ascending ethanol series. Subsequently, bones were embedded in methylmethacrylate and cut into 4-mm sections for staining and 7-mm sections to assess fluorescence labels. The sections were stained with von Kossa and toluidine blue to analyze osteoblast number. Tartrate-resistant acid phosphatase (TRAP) staining was used to identify osteoclasts and unstained sections were analyzed using fluorescence microscopy to determine the mineral apposition rate (MAR) using the two fluorescent labels. Histomorphometric analysis was performed with the Osteomeasure software (OsteoMetrics, Decatur, GA, USA) according to international standards.

Assessment of osteoblast and osteoclast functions

For murine *ex vivo* osteoclast differentiation the *e*piphyseal ends of the femora and tibiae were cut off and the bone marrow was flushed out with DMEM containing 10% fetal calf serum (FCS). Bone marrow stromal cells were collected and plated at a density of 2 x 10^6 cells/cm² in α-MEM containing 10% FCS and 1% penicillin/streptomycin. Following attachment, medium was replaced with basal medium supplemented with macrophage colony-stimulating factor (M-CSF, 25 ng/ml; R & D Systems) for 2 days. Thereafter, cells were cultured for 6 days in differentiation medium containing M-CSF (25 ng/ml) and receptor activator of NF-ĸB ligand (50 ng/ml; R & D Systems). To assess resorption activity, osteoclast precursor cells were plated in resorption pit plates (Osteo Assay Surface 24 well plate, Corning). After 8 days, bone matrix was stained with von Kossa, and the resulting resorption pits were quantified by densitometry.

For murine *ex vivo* osteoblast differentiation, bone marrow stromal cells were differentiated toward osteoblasts using DMEM containing 25 mM of glucose supplemented with 10% FCS, 1% penicillin/streptomycin, 10 nM dexamethasone, 10 mM β-glycerol phosphate, and 100 mM L-ascorbate phosphate.

Human osteoblasts were differentiated from human mesenchymal stem cells (Lonza) using DMEM containing 25 mM of glucose supplemented with 10% FCS, 1% penicillin/streptomycin, 10 nM dexamethasone, 10 mM β-glycerol phosphate, and 100 mM L-ascorbate phosphate.

Mineralization assay and activity of tissue non-specific alkaline phosphatase

Mineralized matrix formation was assessed by Alizarin Red S staining. hSMCs were fixed in 4% paraformaldehyde and stained with 2% Alizarin Red S (pH 4.2, Sigma) for 30 minutes at room temperature (RT). Excess dye was removed by washing the plates with distilled water. Alizarin Red S was eluted from the cell matrix with 100 mM

cetylpyridinium chloride for 20 min at room temperature. Aliquots were taken and measured with a spectrophotometer at 530 nm.

Accumulated calcium in the mineralized matrix from cells and vessels was eluted using 0.6 N hypochloric acid and detected using the Calcium Colorimetric Assay Kit (BioVision, Milpitas, CA, USA).

Tissue non-specific alkaline phosphatase (TNAP) activity was measured in cell cultures and EVs using the Alkaline Phosphatase Activity Colorimetric Assay Kit (BioVision). Both were normalized to the protein concentration.

RNA interference

RNA silencing was performed as described previously (8). Briefly, 50 nM siRNA against sortilin (L-010620), Rab11a (L-004726), Rab11b (L-004727) (all ONTARGETplus SMART-pool, Thermo Scientific, Lafayette, CO, USA), caveolin-1 (s2448, Life Technology), and Fam20C (ID 133024, Life Technology) or non-targeting siRNA (ON-TARGET Non-Targeting Pool, Thermo Scientific) was transferred into SMCs using Dharmafect 1 (Thermo Scientific). Transfection was performed twice per week over the entire cell culture period.

Adenoviral overexpression of sortilin and mutants

Human sortilin (NM_002959.4) ORFEXPRESS™ Gateway® PLUS Shuttle Clone (untagged) was purchased from GeneCopoeia (Rockville, MD, USA). A mutation (either A or D) was introduced at serine 825 using Change-IT multiple mutation site directed mutagenesis kit (USB Ohio, USA). The ViralPower Adenoviral Expression System, together with pAd/CMV/V5-DEST as the destination vector, was used (Life Technologies, Grand Island, NY, USA). The recombination reaction between attL and attR sites was performed using LR Clonase II enzyme mix resulting in pAd/CMV/SORT1. pAd/CMV/V5-GW/*lac*Z was used as control vector. Adenovirus was amplified by transfection of *Pac*I-digested vector in HEK293A cells. Multiplicity of infection (MOI) was determined by Adeno-X Rapid Titer Kit (Clontech, Mountain View, CA, USA). SMCs were transduced with sortilin and control (LacZ) adenoviruses at MOI of 100. For long-term cell culture, transduction was repeated every 7 days.

Overexpression of Fam20c

Fam20c expression vector (pCMV-Entry) was purchased from Origene (Rockville, MD, USA). Tranfection was performed using FugeneHD (Promega). Transfection was repeated twice per week.

Cell viability

Cell viability was assessed using the Cell Titer Blue assay (Promega, Heidelberg, Germany), according to the manufacturer's protocol.

Antibodies

All antibodies were validated by the manufacturer and optimized by the authors.

Protein	Species	Clone number	Vendor	Catalog number	Application
Alkaline Phosphatase, Tissue Non-specific	Human	EPR4477	Novus Biologicals	EPR4477	Western blot
α-SMA	Human	1A4	Dako	M0851	Histology
β-actin	Human, Mouse	AC-15	Novus Biologicals	NB600-501	Western blot
Caveolin-1	Human	-	BD Transduction Laboratories	610406	Immunofluorescence
Caveolin-1	Human	D46G3	Cell Signaling	#3267	Western blot
CD68	Human	KP1	Dako	M0815	Histology
Fam20C	Human	-	Abcam	ab154740	Western blot
LAMP-1	Human	H4A3	Abcam	ab25630	Immunofluorescence
RUNX2	Human		Novus Biologicals	612100	Immunofluorescence
Rab11	Human	D4F5	Cell Signaling	#5589	Western blot
Sortilin	Human	-	Abcam	ab16640	Immunoprecipitation, Histology, Western blot
Sortilin/ Neurotensin Receptor 3	Human	-	BD Transduction Laboratories	612100	Western blot
Sortilin	Mouse	-	R&D Systems	AF2934	Histology

Immunohistochemistry/Immunofluorescence – cells and tissue

Cells were washed with PBS and fixed in 4% paraformaldehyde (Sigma) for 15 minutes, permeabilized for 10 minutes in 0.5% Triton X-100 (Sigma Aldrich), and subsequently washed and blocked with 1% BSA in PBS for 30 minutes. The glass slides were incubated with antibody for sortilin (1:100; abcam, USA), caveolin-1 (1:100; BD), for 2 hours. Alexa Fluor 488-labelled secondary antibody and Alexa Fluor 594-labelled secondary antibody (Life

Technologies) were subsequently applied. After three washing steps, nuclear staining with DAPI (Life Technologies) was performed and slides were covered using a mounting medium (Dako, Glostrup, Denmark).

Tissue samples were cut into 7-µm thin slices, and cryo-sections were fixed in acetone. After blocking in 4% of appropriate serum, sections were incubated with primary antibodies (human sortilin [1:100; abcam]; mouse sortilin [1:100; R&D Systems, Minneapolis, MN, USA]; human α-SMA [1:200, Dako]; and human CD68 [1:200, Dako]), followed by biotin-labeled secondary antibody (Vector Laboratories, Burlingame, CA, USA) and streptavidin-coupled Alexa Fluor 488 antibody (Life Technologies). For immunofluorescence double labeling, after avidin/biotin blocking (Vector Laboratories), the second primary antibody (RUNX2 [1:50; Novus, St. Charles, MO, USA]) was applied overnight at 4º C, followed by biotin-labeled secondary antibody and streptavidin-coupled Alexa Fluor 594 antibody (Life Technologies). Sections were washed in PBS and embedded in mounting medium containing DAPI (Vector Laboratories).

For bright field immunohistochemistry on tissue sections, following the first biotin-labeled secondary antibody incubation, sections were incubated with streptavidin-labeled HRP solution (Dako), followed by AEC solution (Dako). Slides were examined using the Eclipse 80i microscope (Nikon, Melville, NY, USA) or the confocal microscope A1 (Nikon). All images were processed with Elements 3.20 software (Nikon).

Histology

Tissue samples were frozen in OCT compound and 7 µm serial sections were cut. Alkaline phosphatase activity (early marker of osteoblastic differentiation) was detected on unfixed cryosections according to manufacturer instructions (Vector Labs, Burlingame, CA). Von Kossa silver stain was used to visualize inorganic phosphate calcium salts and Alizarin Red to detect calcium deposits. Briefly, for von Kossa staining, section were incubated with 5% silver nitrate (American Master Tech Scientific) for 60 min under UV light, then washed with sodium thiosulfate. Nuclei were stained with nuclear fast red (American Master Tech Scientific). For Alizarin Red, sections were stained with 2% Alizarin Red S (pH 4.2, Sigma) for 30 minutes at room temperature. Excess dye was removed by washing with distilled water. Slides were examined using an Eclipse 80i microscope (Nikon, Melville, NY, USA).”

Fluorescence quantification

Quantification of immunofluorescence and NIRF signal was performed using MatLab. Each image was divided into 250 smaller images. Within each of these portions the total fluorescent signal from each channel was determined and Pearson analysis was used to determine the correlation between each channel.

Labeling of cell compartments and Structure illumination microscopy

CellLight Reagent BacMam 2.0 (Life Technologies) was used to label the *trans*-Golgi network (N-acetylgalactosaminyltransferase 2, GALNT2) and lysosomes (lysosomal associated membrane protein 1, Lamp-1). Human primary coronary artery SMCs were transduced with 30 particles per cell for 24 hours.

Structure illumination microscopy (Zeiss ELYRA Super-Resolution) allowed high resolution imaging of cellular compartments and improves the resolution of traditional optical microscopy down to 100 nm.

RNA preparation and real-time PCR

Total RNA from the cell culture was isolated using TriZol (Life Technologies). Total RNA from the mouse artery was isolated using the RNeasy Micro Kit (Qiagen, Hilden, Germany). Reverse transcription was performed using the QuantiTect Reverse Transcription Kit (Qiagen). The mRNA expression was determined by TaqMan-based real-time PCR reactions (Life Technologies). The following TaqMan probes were used: Hs00361747_m1 (human SORT1), Hs01047978_m1 (human RUNX2), 4326315E (human β-actin), Mm00725448_s1 (mouse Rplp0), Mm00475834_m1 (mouse Alpl) Mm00490905_m1 (mouse Sort1), Mm00725412_s1 (mouse Acta2), and Mm03413826_m1 (mouse Bglap). The expression levels were normalized to β-actin. Results were calculated using the ΔΔCt method, and presented as fold increase relative to control. Human Osteogenesis RT² Profiler™ PCR Array (Qiagen) was used to profile the expression of 84 genes related to osteogenic differentiation.

Western blot analysis

Cells were lysed with RIPA buffer (Thermo Scientific) containing protease and phosphatase inhibitor (Roche). Protein concentration was measured using the bicinchoninic acid (BCA) method (Thermo Scientific). Total protein was separated by 8-12% SDS-PAGE and transferred using the iBlot Western blotting system (Life Technologies). Primary antibodies against human sortilin (1:1,000; Abcam or 1:200; BD), human caveolin-1 (1:1,000; Cell Signaling), human TNAP (1:500, Novus), human Fam20c (1:1,000, Abcam) and human β-actin (1:5,000; Novus)

were used. Protein expression was detected using Pierce ECL Western Blotting substrate Reagent (Thermo Scientific) and ImageQuant LAS 4000 (GE Healthcare, Waukesha, WI, USA).

Immuno-laser capture microdissection (LCM) and RNA amplification

LCM was performed on the Leica LMD6500 Microdissection System. Immunostaining of sortilin was performed as described. Sortilin–positive areas were cut using the following LCM parameters: power, 50 mW; pulse duration, 2 ms; and spot size, 20 Hm. RNA was isolated using using the PicoPure RNA Isoaltion Kit, followed by RNA amplification using the RiboAmp HS Plus RNA Amplification Kit (both Arcturus, Mountain View, CA, USA), according to the manufacturer's protocol. PCR array was performed using the Fluidigm PCR system.

Hydrodynamic analyses of caveolar sortilin content

Caveolae-enriched lipid raft fractions were separated by ultracentrifugation in a discontinuous sucrose gradient system, as reported previously (9). In brief, SMCs from 100-mm dishes were harvested into 1.68 ml of buffer containing 500 mM sodium carbonate (pH 11). The lysates were homogenized (40 strokes in a Dounce homogenizer) and sonicated. The resulting cell suspension was brought to 45% sucrose by adding 90% sucrose (25 mM MES-buffered saline containing 150 mM NaCl). A discontinuous gradient was formed above the 45% sucrose by adding 35% and 5% sucrose solutions (MES-buffered saline containing 250 mM sodium carbonate) and centrifuging at 260,110 g for 18 hours in a MLA-55 rotor (Optima Max Ultracentrifuge, Beckman Coulter, Inc., Brea, CA, USA). Twelve 0.8-ml fractions were collected, starting at the top of each gradient, and an equal volume of each fraction was analyzed by Western blot.

Measurement of cellular free and total cholesterol

Human coronary artery SMCs were cultured for 7 days in control or osteogenic medium. Cells were washed two times in PBS, and then 3:2 hexane:isopropanol (500 µL per well for 6-well dishes or 200 µl for 12-well dishes) was added to the wells and incubated for 1.5 hours at room temperature. The liquid was dried in a vacuum centrifuge to isolate cellular lipids. Cellular protein was quantified using the BCA kit by adding RIPA buffer to the cell layer following the removal of the lipid containing organic solvent. 100 µl isopropanol was added to the dried lipid extracts, and vortexed to solubilize the lipids. Samples were split into two equal fractions and dried in 96-well plates at 37ºC. 20 µL isopropanol was added to each well to solubilize the lipids. Then cholesterol color regent (Wako Free Cholesterol E kit; Wako Life Science INC, Japan) was added to one of the duplicate wells to measure free

cholesterol. The other well received the color reagent containing cholesterol esterase (1 U/mL, Fisher Scientific) to measure total cholesterol. The plate was incubated at 37ºC for 30 minutes and absorption was determined using a multi-well plate reader. Cholesterol content was quantified by generating a standard curve using the standard provided in the Wako kit. Values were normalized to cellular protein content.

Blood Biochemistry

Mouse whole blood was drawn from inferior vena cava into heparinized microtubes and centrifuged at 2,000g for 10 min at 4°C. Plasma was collected and frozen at -80°C. Plasma levels of total cholesterol and triglycerides were measured using commercial kits obtained from Wako Life Science INC, Japan.

Transmission electron microscopy (TEM) and immunogold-labeling on calcified arteries

TEM and immunogold-labeling were performed as previously described (10). Briefly, tissues were immersion-fixed in 2.5% glutaraldehyde, 2% paraformaldehyde, in 0.1 M cacodylate buffer pH 7.4 (modified Karnovsky's fixative). The tissues were dehydrated and embedded in acrylic resin. Thin sections (80 nm) were placed on carbon-coated and glow discharged formvar-coated nickel slot grids. Blocked grids were incubated in primary antibody (Sortilin, Abcam, 1:100) at RT for 1 hour, followed by an appropriate gold-conjugated secondary antibody (goat anti-rabbit 10-nm colloidal gold, 1:25; Abcam) for 1 hour at RT. After fixing with 1% glutaraldehyde in TBS, sections were contrast stained with uranyl acetate. Grids were imaged on a JEOL 1400 TEM equipped with a side mount Gatan Orius SC1000 digital camera.

Co-immunoprecipitation

Cells were lysed in immunoprecipitation (IP) lysis buffer (Thermo Scientific). Sortilin antibody (5 µg, Abcam) or IgG rabbit control antibody (5 µg, Santa Cruz Biotechnology, Santa Cruz, CA, USA) were incubated with Dynabeads Protein G (Life Technologies) by rotation for 2 hours at 4º C followed by washing 3 times with PBS/Tween 20 (0.2%), using a magnet to collect the beads after each wash. 1 mg of protein was pre-cleared by incubation with the bead-bound IgG antibody for 1 hour at 4ºC under rotating conditions. Non-IgG–bound protein was divided and transferred to either bead-bound sortilin antibody or bead-bound IgG antibody, and was incubated for 4 hours at 4ºC under rotating conditions. Bead–antibody–protein complex was washed 3 times with washing buffer (PBS). 90% of the precipitated protein sample was subjected to SDS-PAGE and visualized by Coomassie blue stain (BioRad, Hercules, CA, USA). The prominent band corresponding to the expected molecular weight for sortilin (corroborated

by a parallel Western blot analysis) was excised for in-gel trypsinization. The remaining gel lane for each co-IP condition was divided into eight bands, and in-gel trypsinized (11). Peptides were dissolved in 20 μl of sample loading buffer (0.1 % formic acid, 5 % acetonitrile) for subsequent mass spectrometric analysis.

Cloning and *in vitro* expression of full-length stable isotope-labeled proteins

The human *SORT1* gene was sub-cloned into the N-terminal His tag FLEXIQuant vector (11, 12) and verified by sequencing. Sortilin was *in vitro* transcribed and translated using the CellFree Sciences wheat germ extract system (WEPRO2240H, Cambridge Isotopes), where the translation reaction was carried out in the presence or absence of label, [^{13}C, ^{15}N]-Ser/Thr. Labeled sortilin protein was immuno-purified as described above, and analyzed by mass spectrometry. Phosphorylation of labeled sortilin was observed at three sites including, pS825. Generally, posttranslational modification of *in vitro* standards cannot be completely avoided, although they can be dealt with accordingly when performing relative quantification (11). In this case, we used the wheat germ-incurred pS825 to our advantage as it provided a phosphorylation standard for quantification of pS825 in hSMCs-derived sortilin. Labeled sortilin peptides were then mixed with those from human SMCs or human EVs, according to their respective mass spectrometry signal intensities, in order to achieve a ~1:1 mixing ratio.

Kinase assays using peptide substrate and membrane protein

Fam20c kinase assay was performed as previously described with modifications (13). The sortilin peptide SGYHDDSDEDLLE (amino acids, 819-830) was purchased from New England Peptides. The kinase assay was performed in 50 mM Tris-HCl (ph 7.3), 10mM MnCl, 100 uM ATP, 1mM peptide, 0.5 mg/ml BSA and 1 μg Fam20C or the catalytically inactive form D478A Fam20C for up to 2 hours at 30ºC. Casein kinase 1 and 2 kinase assays were performed according to the manufacture's protocol (New England Biolabs). The peptide was purified using Oasis HLB cartridges (1cc/10mg, Waters, MA, USA) for mass spectrometric analysis using parallel reaction monitoring (PRM).

Kinase assays on sortilin protein - HEK293 cells were transduced with adenovirus-encoding sortilin. Membrane fraction was isolated using the ProteoExtract Transmembrane Protein Extraction Kit (Calbiochem) and membrane buffer A. 3 μg of Fam20C or the catalytically inactive form D478A Fam20C were incubated with 75 μg membrane protein in 50 mM HEPES buffer, 10mM MnCl, 1 mM ATP for 2 hours at 30ºC. Membrane protein without the incubation served as control. Sortilin was then immunoprecipitated as described above. 90% of the precipitated

protein sample was subjected to SDS-PAGE and visualized by Coomassie blue stain. The prominent band corresponding to the expected molecular weight for sortilin (90-110 kDa) was excised for in-gel trypsinization. Peptides were dissolved in 20 μl of sample loading buffer (0.1 % formic acid, 5 % acetonitrile) for mass spectrometric analysis (PRM).

Endogenous kinase activity to phosphorylate sortilin C-terminal peptide

Fam20C was either overexpressed or silenced in calcifying SMCs. Casein kinase 2 was inhibited using 10 μM tetrabromobenzotriazole (TBB). DMSO served as control. After 10 days, SMCs were lysed in RIPA buffer supplemented with phosphatase and protease inhibitors. Kinase assays were performed using 30 μg SMC protein, 1 mM sortilin peptide, SGYHDDSDEDLLE, and 100 uM ATP for 30 min at 30ºC. The sortilin peptide was purified using Oasis column and for mass spectrometric analysis (MS1, area under the cuve based quantification) (12).

Preparation of mouse and human arteries for targeted mass spectrometry, parallel reaction monitoring.

Calcified and non-calcified arteries were isolated from *Apoe*-/- mice (Supplementary Figure 15C). Samples were homogenized in RIPA buffer (plus protease and phosphatase inhibitors). 1 mg of protein was separated on a gel and bands corresonding to the molecular size of sortilin (90-100 kDa) were excised for in-gel trypsinization.

Human carotid artery samples were divided in 2 pieces and homogenized in RIPA buffer (plus protease and phosphatase inhibitors). Sortilin was immunoprecipitated from 1 mg of protein as described above. 90% of the precipitated protein sample was subjected to SDS-PAGE and visualized by Coomassie blue stain. The prominent band corresponding to the expected molecular weight for sortilin (90-110 kDa) was excised for in-gel trypsinization. Peptides were dissolved in 20 μl of sample loading buffer (0.1 % formic acid, 5 % acetonitrile) for mass spectrometric analysis.

Mass spectrometry

Peptide samples were analyzed with either the LTQ-Orbitrap Elite (for co-immunoprecipitation studies) or the Q Exactive mass spectrometer (for FLEXIQuant and FAM20c kinase studies), each fronted with a Nanospray FLEX ion source, and coupled to an Easy-nLC1000 HPLC pump (Thermo Scientific). The peptides were subjected to a dual-column set-up: an Acclaim PepMap RSLC C18 trap column, 75 μm X 20 mm; and an Acclaim PepMap RSLC C18 analytical column 50 μm X 150 mm (Thermo Scientific). The analytical gradient was run at 250 nl/min from

10% to 30% Solvent B (acetonitrile/0.1% formic acid) for 30 minutes, followed by 5 minutes of 95% Solvent B. Solvent A was 0.1% formic acid. All reagents were HPLC-grade. The LTQ-Orbitrap was set at 120 K resolution, and the top 20 precursor ions (within a scan range of 380–2000 *m/z*) were subjected to collision-induced dissociation (collision energy 35%) for peptide sequencing (MS/MS). The dynamic exclusion feature was disabled. The Q Exactive was set to 140 K resolution, and the top 10 precursor ions (within a scan range of 380-2000 *m/z*) were subjected to higher energy collision-induced dissociation (collision energy 27 +/- 10%) for MS/MS. The dynamic exclusion was enabled (20 s). For confirmation of the presence sortilin (phospho-)peptides in SMCs, HEK293 membrane fractions, and in human and mouse calcified and non-calcified tissues, parallel reaction monitoring (resolution = 35K, AGC target = 3e6, maximum IT = 200 ms, isolation window = 3 *m/z,* CE = 27 %) was performed on the Q Exactive using an isolation list comprising the *m/z* and retention times of the selected sortilin peptides sequenced from overexpression studies in SMCs and FLEXIQuant experiments (Supplementary Figure 11). It is important to note that the C-terminal peptide, SGYHDDSDEDLLE, is unique to sortilin when searched against the human and mouse UniProt databases. The identification of the peptides were verified by manually.

Analysis of mass spectrometry data

The MS/MS data were queried against either the human or a modified *Saccharomyces* (containing recombinant Human FLEX-tagged sortilin) UniProt database (downloaded on March 27, 2012) using the SEQUEST search algorithm (14) via the Proteome Discoverer (PD) Package (Thermo Scientific). Methionine oxidation and phosphorylation of Ser and Thr were set as variable modifications, and carbamidomethylation of cysteine was set as a fixed modification. The peptide false discovery rate (FDR) was calculated using Percolator provided by PD; the FDR was determined based on the number of MS/MS spectral hits when searched against the reverse, decoy human or modified *Saccharomyces* database (15, 16). Peptides were filtered based on a 1% FDR, and proteins with three or more unique peptides were analyzed.

For co-immunoprecipitation studies, sortilin–specific proteins were differentiated from non-specific proteins by subtracting the protein hits derived from IgG controls from those of the corresponding sortilin immunoprecipitation. The final co-immunoprecipitation lists include proteins that are completely absent in the IgG samples. For proteins that were present in both sortilin and IgG IPs, but may have been enriched due to sortilin co-immunoprecipitation, only those with peptide-spectrum matches (PSMs) (17) of 20-fold or greater (with respect to the IgG control) were included in the analysis.

For FLEXIQuant, endogenous sortilin peptides were added to a synthesized standard with labeled Ser/Thr for quantitative mass spectrometry analysis (Supplementary Figure 15). In FLEXIQuant, the relative peak profiles of the endogenous sortilin peptides versus their respective *in vitro*-labeled (heavy) variants reflect the relative stoichiometries of sortilin peptides throughout the progression of calcification. MS1 and PRM-based quantification was determined using the Skyline (18) and Xcalibur (Thermo Scientific) software packages.

Supplementary references

1. Xue Y, Liu Z, Cao J, Ma Q, Gao X, Wang Q, Jin C, Zhou Y, Wen L, and Ren J. GPS 2.1: enhanced prediction of kinase-specific phosphorylation sites with an algorithm of motif length selection. *Protein engineering, design & selection : PEDS.* 2011;24(3):255-60.
2. Iwata H, Manabe I, Fujiu K, Yamamoto T, Takeda N, Eguchi K, Furuya A, Kuro-o M, Sata M, and Nagai R. Bone marrow-derived cells contribute to vascular inflammation but do not differentiate into smooth muscle cell lineages. *Circulation.* 2010;122(20):2048-57.
3. Kjolby M, Andersen OM, Breiderhoff T, Fjorback AW, Pedersen KM, Madsen P, Jansen P, Heeren J, Willnow TE, and Nykjaer A. Sort1, encoded by the cardiovascular risk locus 1p13.3, is a regulator of hepatic lipoprotein export. *Cell Metab.* 2010;12(3):213-23.
4. Aikawa E, Aikawa M, Libby P, Figueiredo JL, Rusanescu G, Iwamoto Y, Fukuda D, Kohler RH, Shi GP, Jaffer FA, et al. Arterial and aortic valve calcification abolished by elastolytic cathepsin S deficiency in chronic renal disease. *Circulation.* 2009;119(13):1785-94.
5. Aikawa E, Nahrendorf M, Figueiredo JL, Swirski FK, Shtatland T, Kohler RH, Jaffer FA, Aikawa M, and Weissleder R. Osteogenesis associates with inflammation in early-stage atherosclerosis evaluated by molecular imaging in vivo. *Circulation.* 2007;116(24):2841-50.
6. Yao C, Yao GQ, Sun BH, Zhang C, Tommasini SM, and Insogna K. The transcription factor T-box 3 regulates colony-stimulating factor 1-dependent Jun dimerization protein 2 expression and plays an important role in osteoclastogenesis. *The Journal of biological chemistry.* 2014;289(10):6775-90.
7. Kawano T, Zhu M, Troiano N, Horowitz M, Bian J, Gundberg C, Kolodziejczak K, and Insogna K. LIM kinase 1 deficient mice have reduced bone mass. *Bone.* 2013;52(1):70-82.
8. Goettsch C, Rauner M, Sinningen K, Helas S, Al-Fakhri N, Nemeth K, Hamann C, Kopprasch S, Aikawa E, Bornstein SR, et al. The osteoclast-associated receptor (OSCAR) is a novel receptor regulated by oxidized low-density lipoprotein in human endothelial cells. *Endocrinology.* 2011;152(12):4915-26.
9. Kalwa H, and Michel T. The MARCKS protein plays a critical role in phosphatidylinositol 4,5-bisphosphate metabolism and directed cell movement in vascular endothelial cells. *The Journal of biological chemistry.* 2011;286(3):2320-30.
10. New SE, Goettsch C, Aikawa M, Marchini JF, Shibasaki M, Yabusaki K, Libby P, Shanahan CM, Croce K, and Aikawa E. Macrophage-Derived Matrix Vesicles: An Alternative Novel Mechanism for Microcalcification in Atherosclerotic Plaques. *Circulation research.* 2013.
11. Singh S, Kirchner M, Steen JA, and Steen H. A practical guide to the FLEXIQuant method. *Methods Mol Biol.* 2012;893(295-319.
12. Singh S, Springer M, Steen J, Kirschner MW, and Steen H. FLEXIQuant: a novel tool for the absolute quantification of proteins, and the simultaneous identification and quantification of potentially modified peptides. *Journal of proteome research.* 2009;8(5):2201-10.
13. Tagliabracci VS, Engel JL, Wen J, Wiley SE, Worby CA, Kinch LN, Xiao J, Grishin NV, and Dixon JE. Secreted kinase phosphorylates extracellular proteins that regulate biomineralization. *Science.* 2012;336(6085):1150-3.
14. Yates JR, 3rd, Eng JK, McCormack AL, and Schieltz D. Method to correlate tandem mass spectra of modified peptides to amino acid sequences in the protein database. *Analytical chemistry.* 1995;67(8):1426-36.
15. Elias JE, and Gygi SP. Target-decoy search strategy for increased confidence in large-scale protein identifications by mass spectrometry. *Nature methods.* 2007;4(3):207-14.
16. Kall L, Storey JD, MacCoss MJ, and Noble WS. Assigning significance to peptides identified by tandem mass spectrometry using decoy databases. *Journal of proteome research.* 2008;7(1):29-34.
17. Stevenson SE, Chu Y, Ozias-Akins P, and Thelen JJ. Validation of gel-free, label-free quantitative proteomics approaches: applications for seed allergen profiling. *Journal of proteomics.* 2009;72(3):555-66.

18. MacLean B, Tomazela DM, Shulman N, Chambers M, Finney GL, Frewen B, Kern R, Tabb DL, Liebler DC, and MacCoss MJ. Skyline: an open source document editor for creating and analyzing targeted proteomics experiments. *Bioinformatics.* 2010;26(7):966-8.